

# Fractionation of the Isotopes of Carbon and Hydrogen in Biosynthetic Processes\*

John M. Hayes (jhayes@whoi.edu)

National Ocean Sciences Accelerator Mass Spectrometry Facility and Department of Geology and Geophysics, Woods Hole Oceanographic Institution, Woods Hole, MA 02543, USA

Chapter prepared for a short course sponsored by the Mineralogical Society of America and organized by John W. Valley and David R. Cole. Presented at the National Meeting of the Geological Society of America, Boston, MA, 2-4 November 2001. This pdf can be downloaded from [nosams.whoi.edu/jmh/](http://nosams.whoi.edu/jmh/).

This review is concerned with the isotopic relationships between organic compounds produced by a single organism, specifically their enrichments or depletions in  $^{13}\text{C}$  relative to total-biomass carbon. These relationships are biogeochemically significant because

(1) An understanding of biosynthetically controlled, between-compound isotopic contrasts is required in order to judge whether plausibly related carbon skeletons found in a natural mixture might come from a single source or instead require multiple sources.

(2) An understanding of compound-to-biomass differences must underlie the interpretation of isotopic differences between individual compounds and total organic matter in a natural mixture.

My approach is pedagogic. The coverage is meant to be thorough, but the emphases and presentation have been chosen for readers approaching this subject as students rather than as research specialists. In common with the geochemists in my classes, many readers of this paper may not be very familiar with biochemistry and microbiology. I have not tried to explain every concept from those subjects and I have not inserted references for points that appear in standard texts in biochemistry or microbiology. Among such books, I particularly recommend the biochemistry text by Garrett and Grisham (1999) and the microbiology text by Madigan *et al.* (2000). The biochemistry text edited by Zubay (1998) is also particularly elegant and detailed. White (1999) has written a superb but condensed text on the physiology and biochemistry of prokaryotes.

A schematic overview of the relevant processes is shown in Figure 1. Plants and other autotrophs fix  $\text{CO}_2$ . Animals and other heterotrophs utilize organic compounds. If the assimilated carbon is a small molecule (like  $\text{CO}_2$ ,  $\text{CH}_4$ , or acetate), significant isotopic fractionation is likely to accompany the fixation or assimilation of C. Such fractionations establish the isotopic relationship between an

organism and its carbon source. Those associated with photosynthesis encode information about chemical and physical conditions in the environment of fixation. Logically, therefore, they are treated here in the chapter dealing with the biogeochemistry of marine basins (Freeman, this volume).

The initial products formed by autotrophs are small carbohydrates (“the photosynthate”). In heterotrophs, if a carbon skeleton is not destined for incorporation in biomass with little or no alteration, it is commonly broken down to yield two- and three-carbon “metabolic intermediates.” Depending on whether we’re talking about an autotroph or a heterotroph, either the small carbohydrates or the metabolic products then serve as inputs to downstream processes. These involve oxidation, reduction, bond formation, and bond cleavage. Some of these processes produce energy and others consume it. They are balanced against each other, and the organism will remain viable as long as net yields of energy are adequate for maintenance. Growth – the production of additional biomass – will be possible if photosynthate or metabolites remain after adequate quantities of energy have been produced. This will depend not only on the magnitude of the supply but also on the range of ener-

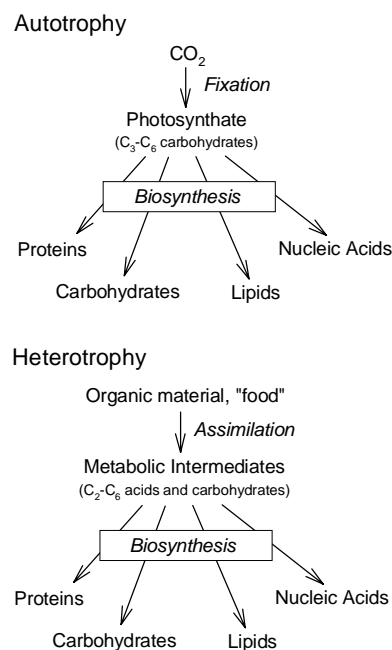
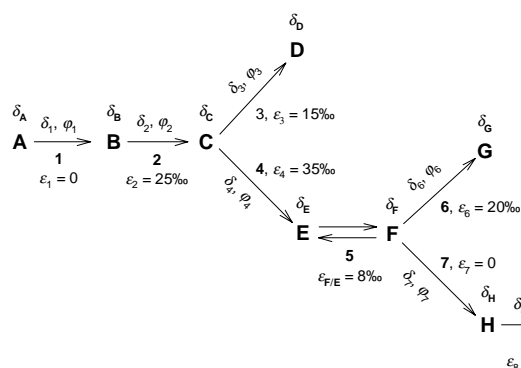


Figure 1. The roles of biosynthesis in autotrophic and in heterotrophic organisms.

\* Dedicated to my father and mother on his 90<sup>th</sup> birthday and their 65<sup>th</sup> wedding anniversary, 26 March 2001. Of all the good fortunes that I have enjoyed, none equals that of being his son and their child.



**Figure 2.** A network of chemical reactions. Letters indicate carbon positions within reactants and products. Isotopic compositions of these positions are indicated by  $\delta$ s with alphabetical subscripts. Reactions are designated by numbers and the  $\delta$ s,  $\phi$ s, and  $\epsilon$ s with numerical subscripts indicate respectively isotopic compositions of the carbon being transmitted by a reaction, the flux of carbon being transmitted (moles/time), and the isotope effect associated with the reaction. The latter value is expressed in ‰ and  $\epsilon$  is defined in the text accompanying equation 1.

gy-producing processes accessible (for example, whether the availability of  $O_2$  permits aerobic respiration). Remaining supplies, and the mixture of further energy-producing and energy-consuming processes, will then be managed so that a portion of the available carbon flows through the network of reactions required to produce the mixture of nucleic acids, proteins, carbohydrates, and lipids that together form biomass. It is the isotopic budget for that reaction network that concerns us here.

## Isotopes in Reaction Networks

### Isotope effects and mass balance

An arbitrary sequence of reactions is indicated schematically in Figure 2. Analysis of this system will provide a useful introduction to studies of real organisms. Reactant **A** could, for example, represent a particular carbon position in a two- or three-carbon product of metabolism or photosynthesis. If there were no isotope effect associated with reaction 1 ( $\epsilon_1 = 0$ ), then the isotopic composition of the carbon being transmitted by reaction 1 would be equal to that of reactant **A**. This follows from a general relationship<sup>1</sup> which can be written as

$$\delta_p = \delta_r - \epsilon \quad (1)$$

where  $\delta_p$  and  $\delta_r$  are the instantaneous isotopic compositions of a product and reactant and  $\epsilon$  (expressed in ‰) is the isotope effect associated with the reaction linking R and P. Here we have  $\delta_1 = \delta_A - \epsilon_1$  and, from  $\epsilon_1 = 0$ ,  $\delta_1 = \delta_A$ . To provide a quantitative basis for downstream  $\delta$  values, we will define  $\delta_A = 0\text{‰}$ .

<sup>1</sup> In order to focus on the principles, we will adopt the approximation represented by equation 1. The precise relationship, which should be used in order to avoid errors in practical work, is given by  $\epsilon \equiv 10^3(\alpha - 1)$ , where  $\alpha \equiv [(\delta_r + 1000)/(\delta_p + 1000)]$ .

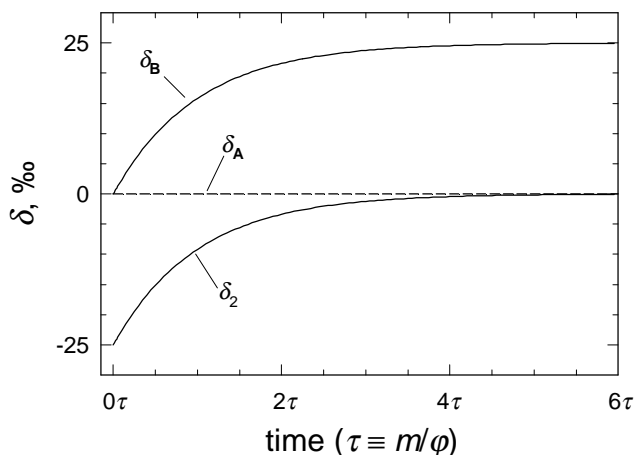


**Figure 3.** Isotopic compositions as a function of time. Time is expressed in units of  $\tau$ , the time constant for the system. As noted,  $\tau = m/\phi$ , where  $m$  is the quantity of intermediate present at steady state. Values of  $\delta$  refer to reactant **A** (broken line), product **B** (upper solid line), and the carbon transmitted by reaction 2 (lower solid line).

The example depicted in Figure 2 indicates that **B** is an intermediate between **A** and **C**. There is no division of the carbon flow, but there is a significant isotope effect associated with reaction 2, which transforms **B** to yield **C**. Two requirements then seem to collide. From equation 1, we know that  $\delta_2 = \delta_B - \epsilon_2$ . From conservation of mass we have  $\delta_2 = \delta_1$ . Since  $\epsilon_2 = 25\text{‰}$ , this requires  $\delta_B = +25\text{‰}$  even though  $\delta_1$  (the  $d$  value of the carbon flowing to **B**) =  $0\text{‰}$ . At steady state, this *must* be true. Initially, it *cannot* be. The resolution of these requirements is shown in Figure 3, which depicts isotopic compositions as a function of time. Initially  $\delta_1 = 0$  and  $\delta_2 = -25\text{‰}$ . As a result of this imbalance,  $\delta_B$  rises until  $\delta_2 = \delta_1$ . The time constant for an adjustment of this kind is given by  $\tau = m/\phi$ , where  $m$  represents the quantity of the intermediate (**B** in this case) present at steady state and  $\phi$  is the flux (*e. g.*, moles/time) of material through the intermediate pool. Whenever standing stocks are small relative to throughputs, steady-state conditions must be dominant in biosynthetic-reaction networks.

The flow of carbon divides at **C**, which lies at branch point in the network. From equation 1 and the isotope effects specified for reactions 3 and 4, we have  $\delta_3 = \delta_C - 15\text{‰}$  and  $\delta_4 = \delta_C - 35\text{‰}$ . Mass balance requires also that the total amounts of  $^{12}\text{C}$  and  $^{13}\text{C}$  flowing to and from **C** are equal. In mathematical terms, the mass balance for total carbon is specified by

$$\phi_2 = \phi_3 + \phi_4 \quad (2)$$

The mass balance for carbon-13 is specified by

$$\phi_2 \delta_2 = \phi_3 \delta_3 + \phi_4 \delta_4 \quad (3)$$

At steady state, the flux terms can be replaced by a coefficient that describes the division of the carbon flow in terms of a branching ratio,  $f_3 \equiv \phi_3/\phi_2$ , where  $f_3$  is the fraction of

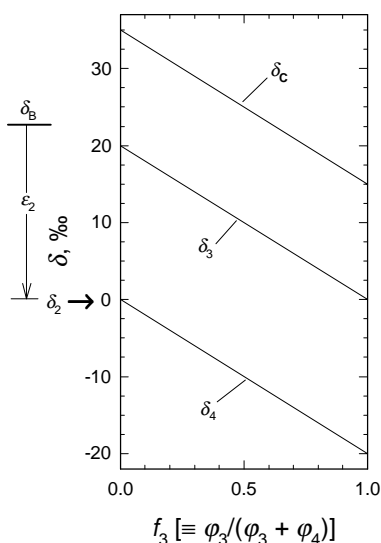


**Figure 4.** Isotopic compositions of carbon flows, and of reactant **C**, at the **C** branch point. As shown by the graph, values of  $\delta$  vary with  $f_3$ , a parameter equivalent to the fractional yield of **D**. The zero point of the  $\delta$  scale is arbitrarily set by the isotopic composition of the input carbon flow,  $\delta_1$ . The diagram at the left of the graph indicates  $\delta_2$ , the isotopic composition of the carbon flowing to the branch point, and its relationship to  $\delta_B$ .

also that the *yield* of **D**, a byproduct in this reaction network, could have an important effect on  $\delta_1$ .

The appearance of graphs like Figure 4 is controlled largely by the relative magnitudes of the isotope effects. The lines representing the isotopic compositions of the branching flows will be separated vertically by the difference between the isotope effects. If  $f$  expresses the fraction of the depleted product, the lines will have a positive slope. The slope will be negative if  $f$  expresses the fraction of the enriched product (compare Figures 4 and 5).

Substances **E** and **F** are in equilibrium. As a result, their isotopic compositions will vary together, the difference being controlled by the isotope effect associated with the equilibrium. In the example depicted by Figure 2, **F** will always be enriched in  $^{13}\text{C}$  by 8‰ relative to **E**. The branch point at **F** is similar to that at **C**. In this case, the absence of an isotope effect at reaction 7 means that the carbon flowing to **H** will have an isotopic composition equal to that of **F**, but the presence of a branching pathway with an unequal isotope effect ( $\epsilon_6 \neq \epsilon_7$ ) means that significant fractionation can still occur. The resulting isotopic relationships are summarized graphically in Figure 5 and show that **G** provides a second example of a byproduct whose yield can influence the isotopic composition of **I**.

A substantial isotope effect is associated with reaction 8, but the absence of a branching pathway means that the isotopic composition of **I** is effectively controlled by  $\delta_7$  ( $\delta_1 = \delta_7$ ). The only effect of  $\delta_8 > 0$  is to require that, at steady

**C** that flows through reaction 3 to yield **D**.

$$\delta_2 = f_3 \delta_3 + (1 - f_3) \delta_4 \quad (4)$$

The resulting relationship, in which the isotopic composition of the carbon flowing to **D** and **E** depends on  $f_3$ , is summarized graphically in Figure 4. As shown, at steady state, **C** can be either enriched or depleted in  $^{13}\text{C}$  relative to **B**.

Isotopic shifts imposed on **E** propagate downstream. As a result, the isotopic compositions of **E**, **F**, **G**, **H**, and **I** are all affected by  $f_3$ . Any investigator seeking to understand the isotopic composition of **I**, and perhaps focusing his or her attention on reactions 1, 2, 4, 5, 7, and 8 (the pathway linking **A** and **I**), would have to remember

state, **H** is enriched relative to **I**.

### Carbon positions vs. whole molecules

Important words appear in the caption to Figure 2: “Letters indicate carbon positions within reactants and products.” For example, **C** could represent the C-2 (carbonyl) position in pyruvate. **D** and **E** would then represent the fates of that position in products derived from the pyruvate. Reactions occur between molecules but isotopic selectivity is expressed as chemical bonds are made or broken at particular carbon positions. Isotope effects pertain to those specific processes and control fractionations only at the

reaction site, not throughout the molecule. To calculate changes in the isotopic compositions of whole molecules, we must first calculate the change at the reaction site, then make allowance for the rest of the molecule. In doing so, we inevitably find that the site-specific isotopic shift is diluted by admixture of the carbon that was just along for the ride. It follows that the isotopic differences that can be observed *between* molecules “must be related to, indeed, must be the attenuated and superficial manifestations of, isotopic differences *within* molecules” (Monson and Hayes, 1982a).

### Useful lessons

Generalities can be drawn from the foregoing discussion. First, isotopic compositions of intermediates (*e. g.*, **B**) can differ substantially from those of final products (*e. g.*, **I**). Second, the division of carbon flows at branch points can strongly affect isotopic compositions downstream. As a result, it is practically impossible to predict the isotopic compositions of final, biosynthetic products on the basis of observed isotopic compositions of intermediates. In plain words, if you want to know about the isotopic composition of lipids, it’s very risky to rely entirely on analyses of acetate, even though most lipids are produced from acetate.

On the other hand, if you want to know, for example, *why* lipids are depleted in  $^{13}\text{C}$  relative to other biosynthetic products, it will be necessary to examine evidence capable of revealing the structure and characteristics of the related network of reactions. Two complementary approaches have been developed thus far. Most straightforwardly, DeNiro and Epstein (1977) devised experiments for the

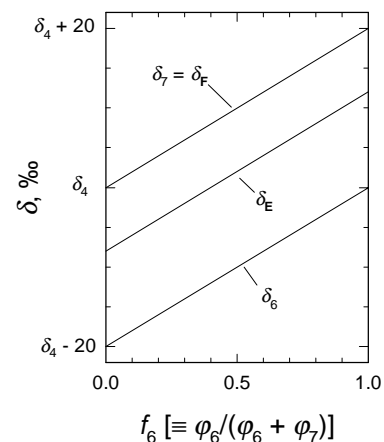


**Figure 5.** Isotopic compositions of carbon flows, and of components of the **E-F** equilibrium, at the **F** branch point. Values of  $\delta$  vary with  $f_6$ , the fractional yield of **G**, and are expressed relative to  $\delta_4$ , the isotopic composition of the carbon flowing to the **E** ⇌ **F** equilibrium. Values of  $\delta$  shown on this graph cannot be expressed relative to  $\delta_1$  unless  $f_3$  has been specified (see Fig. 4, which shows that  $\delta_4$  is a function of  $f_3$ ).

determination of isotope effects at key points in the reaction network that links *n*-alkyl lipids to metabolites derived from carbohydrates and from some amino acids. In contrast, Abelson and Hoering (1961) pioneered the examination of intramolecular patterns of isotopic order. They studied the biosynthesis of amino acids, analyzing only the end products. However, they determined not only the  $\delta$  values of the individual molecules but also (to the extent possible) the distributions of  $^{13}\text{C}$  *within* the molecules. A similar approach was later used by Monson and Hayes (1982a) to study isotopic fractionations in lipid biosynthesis.

These reaction-based and product-based lines of investigation are complementary because neither can be perfect or complete and because inferences drawn from their results must be consistent. Even if it were possible to determine the isotope effect at each carbon position for every single step in a reaction sequence, and even if it were possible to recognize in advance every significant feature of the network, it would never be possible to be sure that studying the reactions in isolation was a reliable guide to their characteristics *in vivo*. On the other hand, even if it were possible to determine the isotopic composition at every single carbon position within all the related products of a network, it would never be possible to assign each observed variation reliably to causes that might lie many steps upstream in the sequence of reactions. More positively, results of intramolecular isotopic analyses could show that reaction-based investigations must have overlooked a key step. And, if multiple reaction steps have significantly influenced isotopic compositions in end products, quantitative interpretation of intramolecular patterns of isotopic order requires information developed from reaction-based studies. Examples will be provided in subsequent sections of this review.

## Further General Factors Affecting Isotopic Compositions

### Compartmentalization

A cell is not a stirred reaction vessel. In eukaryotic algae, for example,  $\text{CO}_2$  is fixed and initial carbohydrates are produced in the chloroplast (also called plastid). Fatty acids are produced in the chloroplast and then exported for use elsewhere in the cell (Ohlrogge and Jaworski, 1997) and all of the  $\text{C}_{20}$  and  $\text{C}_{40}$  isoprenoid carbon skeletons required by the photosynthetic apparatus are plastidic products (Kleinig, 1989). In contrast, sterols, which are derived from a  $\text{C}_{30}$  isoprenoid carbon skeleton, are produced in the cytosol (Lichtenthaler, 1999). In higher plants, the carbon feedstocks required to support biosynthesis outside the chloroplast are exported mainly as the  $\text{C}_3$  carbohydrate derivative, dihydroxyacetone phosphate (Schleucher *et al.*, 1998). As a result of these factors, plastidic fatty acids and cytosolic sterols, both derived from acetate, can have different isotopic starting points. Moreover, even when starting points and downstream processes are closely similar, the separation of pathways between compartments can

mean that divisions of carbon flows at branch points differ significantly and, therefore, that final isotopic compositions differ sharply.

Smaller and larger organisms can present correspondingly simpler and more complex isotopic relationships. Prokaryotic cells, those of Archaea and Bacteria, are much smaller and lack the internal boundaries that stabilize chemical compartmentalization in Eukarya. As a result, compounds with similar structures and deriving from the same biosynthetic pathway *usually* have similar isotopic compositions (but see “Timing,” below). In contrast, for higher organisms with differentiated cells, it is entirely possible that two compounds with identical carbon skeletons and biosynthetic origins (same pathway of synthesis, same location within the cell) but from different cell types (leaf epidermis *vs.* palisade cell) would have very different isotopic compositions even though both were products of the same organism.

### Timing and reversibility

The concept of steady state was stressed in the discussion of Figures 2-5. But even bacterial populations have phases of growth (lag, exponential, stationary, and death) and, within a single cell, the production of one or more enzymes need not be uniform over the life of a cell. As a result, isotope effects at one or more important branch points may change. If an enzyme with a small isotope effect substitutes for one with a large effect, the isotopic compositions of downstream products will change. A specific example of this has been identified in methanotrophic bacteria (Summons *et al.*, 1994) and is discussed in a concluding section of this review.

Reversibility of carbon flows must also play a role in controlling isotopic compositions of biosynthetic products. If carbon flows only *to* a particular product, it will be necessary only to consider isotope effects and branching ratios on the synthetic pathway. On the other hand, the isotopic compositions of compounds that are constantly being degraded as well as produced – compounds which “turn over” within the organism – will be shaped in addition by the isotopic characteristics of the degradative processes. Moreover, the *degree* of reversibility will be important. Molecular catalysts for which needs change over the lifetime of an organism – enzymes – turn over rapidly. Structural components such as lignin, cellulose, and some proteins (built from the same amino acids also found in enzymes) turn over much more slowly. There is evidence that the flow of carbon to the fatty acids in bacterial membranes is essentially unidirectional (Cronan and Vagelos, 1972) and that some fatty acids involved in the regulation of membrane fluidity in higher plants turn over quite rapidly (Monson and Hayes, 1982b), perhaps in response to diurnally cycling temperatures.

## Isotopic Compositions of Compound Classes Relative to Biomass

The most basic sorting of isotopes occurs in the distri-

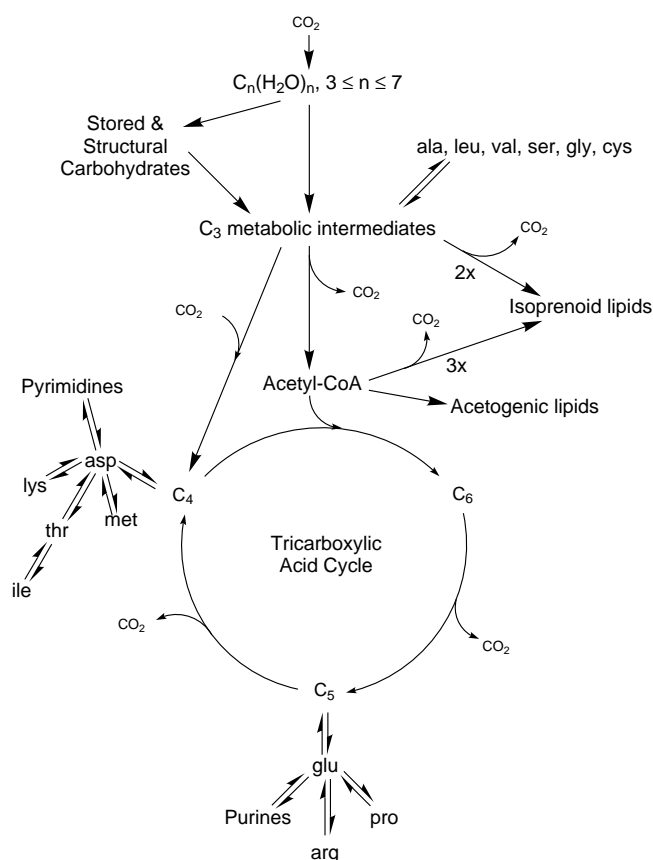


**Figure 6.** An overview of metabolic relationships. The arrows indicate dominant directions of carbon flow in, for example, a growing algal unicell. Most of the pathways indicated are, however, found in nearly all living organisms and are reversible to some degree. The three-letter abbreviations designate amino acids and are decoded in Table 1. As indicated, isoprenoid lipids can be made from either  $C_2$  (acetyl-CoA) or  $C_3$  precursors (see discussions of Table 4 and Figure 29). The reversibility of the pathways related to the amino acids is indicated explicitly because those compounds turn over most rapidly and in practically all organisms.

tribution of carbon among nucleic acids, proteins, carbohydrates, and lipids, the major classes of compounds present within most cells. The most important pathways of carbon flow are indicated schematically in Figure 6. In autotrophs, these lead from carbohydrates (the direct products of carbon fixation) to proteins, nucleic acids, and lipids. Biomass – the organic material that comprises a living organism – is a mixture of these products. Two kinds of isotopic relationships are often discussed, those between various classes (*e. g.*, “lipids are depleted in  $^{13}\text{C}$  relative to proteins”) and those between classes and biomass (*e. g.*, “abundances of  $^{13}\text{C}$  in nucleic acids and in biomass are essentially equal”). The first of these comparisons expresses a relationship like that between  $\delta_3$  and  $\delta_4$  in Figure 4. As carbon flows either to lipids or to proteins, we can expect the isotopic difference between them to remain roughly constant even though the  $\delta$  values themselves will change. That change occurs *relative to* the available carbon supply ( $\delta_2$  in Fig. 4). Such changes must affect class-

Table 1. Abbreviations for Amino Acids<sup>a</sup>

Amino Acid	Single-Letter Code	Three-Letter Code	Amino Acid	Single-Letter Code	Three-Letter Code
Alanine	A	ala	Isoleucine	I	ile
Arginine	R	arg	Leucine	L	leu
Aspartic acid	D	asp	Lysine	K	lys
Asparagine	N	asn	Methionine	M	met
asp and/or asn		asx	Phenylalanine	F	phe
Cysteine	C	cys	Proline	P	pro
Glutamic acid	E	glu	Serine	S	ser
Glutamine	Q	gln	Threonine	T	thr
glu and/or gln		glx	Tryptophan	W	trp
Glycine	G	gly	Tyrosine	Y	tyr
Histidine	H	his	Valine	V	val

<sup>a</sup> The more compact and less memorable single-letter codes are widely used in molecular biology and in proteomics. Most biogeochemical papers are still using the three-letter codes and this review follows that precedent.

to-biomass comparisons. If more carbon flows to lipids, the cell will become more lipid-rich and its isotopic composition will approach that of the lipids. The depletion of  $^{13}\text{C}$  in the lipids, expressed relative to biomass rather than relative to proteins, will decrease. This phenomenon can be considered quantitatively.

The isotopic composition of biomass carbon is given by equation 5.

$$\delta_{\text{Biomass}} = X_{\text{CNA}} \delta_{\text{NA}} + X_{\text{CProt}} \delta_{\text{Prot}} + X_{\text{CSacc}} \delta_{\text{Sacc}} + X_{\text{CLip}} \delta_{\text{Lip}} \quad (5)$$

where the subscripts NA, Prot, Sacc, and Lip respectively refer to nucleic acids and related materials such as nucleoside cofactors, proteins and amino acids, mono- and polysaccharides, and lipids of all kinds. The  $X_C$  terms, which sum to 1.0, refer to mole fractions of carbon and the  $\delta$  terms refer to mass-weighted average isotopic compositions for all of the compounds within the indicated classes. Referring specifically to marine phytoplankton and considering a wide range of available observations, Laws (1991) concluded that  $X_{\text{CProt}}/X_{\text{CNA}} = 8.6$  and discussed further regularities: at maximal rates of growth,  $X_{\text{CProt}}$  approaches 0.54; if the rate of growth is limited by availability of nutrients,  $X_{\text{CProt}}$  declines to values as low as 0.15 (with parallel declines in  $X_{\text{CNA}}$ ); at low light levels,  $X_{\text{CSacc}}$  increases relative to  $X_{\text{CLip}}$ .

Regularities prevail also in isotopic relationships. Isotopic compositions of compound classes reported by Blair *et al.* (1985), Coffin *et al.* (1990), Benner *et al.* (1987), and Sternberg *et al.* (1986) converge to yield estimates of  $\delta_{\text{NA}} \approx \delta_{\text{Prot}} \delta_{\text{Prot}} - \delta_{\text{Sacc}} \approx -1\%$ , and  $\delta_{\text{Lip}} - \delta_{\text{Sacc}} \approx -6\%$ . Figure 7, which expresses the depletion of  $^{13}\text{C}$  in lipids relative to biomass, has been prepared using these relationships and equation 5. *Note:* the indicated depletions have been

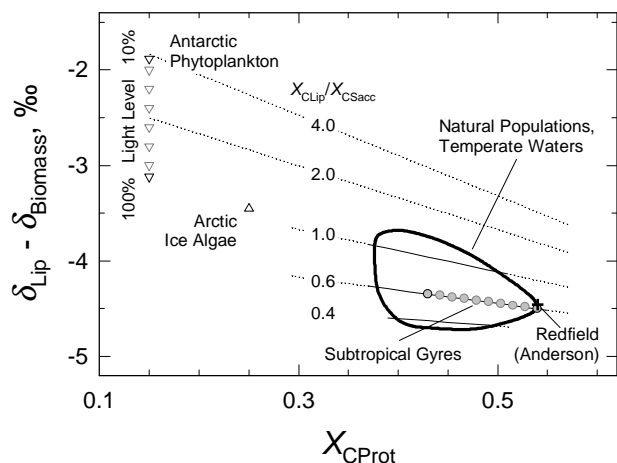


**Figure 7.** The depletion of  $^{13}\text{C}$  in lipids relative to biomass as a function of cellular composition, where  $X_{\text{CProt}}$ ,  $X_{\text{CLip}}$ , and  $X_{\text{CSacc}}$  are the mole fractions of carbon in proteins, lipids, and carbohydrates, respectively (see equation 5 and related discussion). The indicated relationships are based on isotopic mass-balance requirements and on concepts outlined by Laws (1991). The cross marked “Redfield (Anderson)” indicates the position of cells with C/N/P = 106/16/1 but with lower (and much more realistic) abundances of H and O than those specified by the conventional Redfield formula (Anderson, 1995).

calculated, not measured. The intent is to illustrate and to consider factors controlling  $\delta_{\text{Lip}} - \delta_{\text{Biomass}}$ . If the saccharide-to-lipid fractionation in a particular organism were appreciably different from -6‰, the vertical axis would expand or contract. The results show both that the depletion of lipids in  $^{13}\text{C}$  relative to biomass *can* vary widely and that, in nature, a consistent depletion can be understood quite readily. The dotted and solid lines represent relationships between the isotopic depletion and  $X_{\text{CProt}}$  at varying values of the lipid/carbohydrate ratio ( $X_{\text{CLip}}/X_{\text{CSacc}}$ ). They show that the isotopic depletion becomes more marked as lipids become less abundant (*i. e.*, as  $X_{\text{CProt}}$  increases) and that the relative abundance of carbohydrates can also be an important controlling factor.

The biomass of phytoplankton successfully competing in marine environments generally falls within the area enclosed by the gray envelope (Laws, 1991). Compositions can vary more widely in laboratory cultures and in some extreme environments. The range which has been observed is roughly indicated by the extent of the dotted lines and by the points and ranges indicated for Arctic and Antarctic phytoplankton (Laws, 1991 and references therein). For the particular case of phytoplankton in subtropical gyres, Laws (1991) estimates values of  $X_{\text{CProt}}$  and  $X_{\text{CLip}}/X_{\text{CSacc}}$  in the range indicated by the open circles. The maximum-protein end of this range lies close to the composition derived by Anderson (1995) as an updated and improved estimate of the Redfield composition ( $\text{C}_{106}\text{H}_{175}\text{O}_{42}\text{N}_{16}\text{P}$  instead of  $\text{C}_{106}\text{H}_{263}\text{O}_{110}\text{N}_{16}\text{P}$ ).

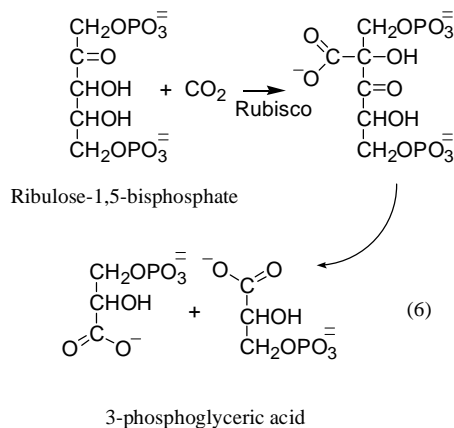
## Isotopic Compositions of Carbohydrates

### Mechanisms of production

Organic carbon is depleted in  $^{13}\text{C}$  relative to inorganic carbon largely because of isotopic fractionations associated with the fixation of  $\text{CO}_2$ . Moreover, some of the hydrogen incorporated in this process becomes the first non-exchangeable H that shapes the hydrogen isotopic composition of organic materials.

Not all carbon fixation is photosynthetic. Table 2 provides an overview that has been organized in terms of the substrates, enzymatic catalysts, and first stable products. It does not include all processes in which inorganic carbon is incorporated in organic molecules, but it is meant to include all processes that contribute to net carbon fixation in organisms that can grow autotrophically. It thus includes pathways that occur not only in plants but also in Bacteria and Archaea that build biomass from inorganic carbon while deriving energy from chemical reactions.

For the moment, we will focus on photoautotrophs that utilize rubisco. Rubisco is the official name of an enzyme for which the systematic name – ribulose-1,5-bisphosphate carboxylase oxygenase – is inconveniently long. As indicated by the first activity specified in the systematic name, this enzyme catalyzes the carboxylation of ribulose-1,5-bisphosphate, “RuBP,” a five-carbon molecule. A six-carbon product is formed as a transient intermediate, but the first stable products are two molecules of “PGA,” 3-phosphoglyceric acid,  $\text{C}_3\text{H}_7\text{O}_7\text{P}$ . The carbon number of this compound gives the process its shorthand name, “ $\text{C}_3$  photosynthesis.” At physiological pH, the acidic functional groups on the reactants and products are ionized as shown below.



This reaction fixes carbon but there is no net change in oxidation number. The  $\text{CO}_2$  is reduced to carboxyl but one of the carbon atoms in the RuBP is oxidized to yield the second carboxyl group. In subsequent steps, each mole of PGA reacts with a mole of NADPH in order to produce two moles of 3-phosphoglyceric acid, a product in which average oxidation number of carbon is 0. NADPH is the reduced form of nicotinamide adenine dinucleotide phosphate (see any biochemistry text for structures and further details). In biosynthetic processes, it functions as a hy-

Table 2. Enzymatic isotope effects and overall fractionations associated with fixation of inorganic carbon during autotrophic growth

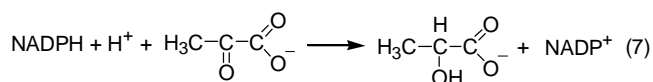
Pathway, enzyme <sup>a</sup>	Reactant and substrate	Product	$\epsilon^b$ , ‰	Notes
<b>C<sub>3</sub></b>			10-22	1
Rubisco, form I, green plants and algae	CO <sub>2</sub> + Ribulose-1,5-bisphosphate	3-Phosphoglyceric acid (two moles)	30	2
Rubisco, form II, bacteria and cyanobacteria	CO <sub>2</sub> + Ribulose-1,5-bisphosphate	3-phosphoglyceric acid (two moles)	22	3
Phosphoenolpyruvate (PEP) carboxylase	HCO <sub>3</sub> <sup>-</sup> + PEP	Oxaloacetate	2	4
PEP carboxykinase	CO <sub>2</sub> + PEP	Oxaloacetate		5
<b>C<sub>4</sub> and CAM</b>			2-15	6
Phosphoenolpyruvate (PEP) carboxylase	HCO <sub>3</sub> <sup>-</sup> + PEP	Oxaloacetate	2	4
Rubisco, form I, green plants and algae	CO <sub>2</sub> + Ribulose-1,5-bisphosphate	3-Phosphoglyceric acid (two moles)	30	1
<b>Acetyl-CoA</b>			15-36	7
Formate dehydrogenase	CO <sub>2</sub> + 2 [H]	HCO <sub>2</sub> <sup>-</sup>		
Carbon monoxide dehydrogenase	CO <sub>2</sub> + 2 [H] + H <sub>4</sub> Pt-CH <sub>3</sub> + CoASH	CH <sub>3</sub> COSCoA + H <sub>2</sub> O + H <sub>4</sub> Folate	52	8
Pyruvate synthase	CO <sub>2</sub> + Acetyl-CoA + 2 [H]	Pyruvate + CoASH		9
PEP carboxylase	HCO <sub>3</sub> <sup>-</sup> + PEP	Oxaloacetate	2	3
PEP carboxykinase	CO <sub>2</sub> + PEP	Oxaloacetate		10
<b>Reductive or reverse TCA Cycle</b>			4-13	11
$\alpha$ -Ketoglutarate synthase	CO <sub>2</sub> + Succinyl-CoA	$\alpha$ -Ketoglutarate + CoASH		
Isocitrate dehydrogenase	CO <sub>2</sub> + $\alpha$ -Ketoglutarate + 2 [H]	Isocitrate		
Pyruvate synthase	CO <sub>2</sub> + Acetyl-CoA + 2 [H]	Pyruvate + CoASH		
PEP carboxylase	HCO <sub>3</sub> <sup>-</sup> + PEP	Oxaloacetate		
<b>3-Hydroxypropionate Cycle</b>			0	12
Acetyl-CoA carboxylase	HCO <sub>3</sub> <sup>-</sup> + Acetyl-CoA	Malonyl-CoA		
Propionyl-CoA carboxylase	HCO <sub>3</sub> <sup>-</sup> + Propionyl-CoA	Methylmalonyl-CoA		
unknown		→ C <sub>3</sub>		13
unknown		→ C <sub>4</sub>		13

<sup>a</sup> For the C<sub>3</sub> and C<sub>4</sub> pathways, the enzymes are listed in the order in which they process carbon. For the bacterial pathways, the enzymes are listed in order of their quantitative contributions to net carbon fixation.

<sup>b</sup>  $\equiv 1000[(^{12}\text{C}/^{13}\text{C}) - 1]$ . Values of  $\epsilon$  reported for pathways rather than for specific, enzymatic reactions reflect overall fractionation of <sup>13</sup>C vs. CO<sub>2</sub> and must represent a weighted average of the related enzymatic isotope effects.

**Notes.** 1. The tabulated range is an estimate chosen to include both tropical phytoplankton with  $\delta \approx -18\text{‰}$  and land plants with  $\delta \approx -30\text{‰}$ . 2. Guy *et al.*, 1993; also reported as 29‰, Roeske and O'Leary, 1984. 3. Guy *et al.*, 1993; also reported as 18‰, Roeske and O'Leary, 1985. 4. O'Leary *et al.*, 1981. PEP carboxylase maintains supplies of C<sub>4</sub> metabolic intermediates (= *anaplerotic* fixation) during growth of C<sub>3</sub> plants and many bacteria. In C<sub>4</sub> plants it fulfills the same function *and* catalyzes the initial C-fixing reaction. 5. According to Descolas-Gros and Fontugne (1990), PEP carboxykinase is the main anaplerotic producer of C<sub>4</sub> intermediates in diatoms and chrysophytes. 6. The tabulated range is an estimate including both C<sub>4</sub> plants with  $\delta \approx -10\text{‰}$  and CAM plants with  $\delta \approx -23\text{‰}$ . 7. Preuß *et al.* (1989); Belyaev *et al.* (1983). 8. Gelwicks *et al.* (1989), isotope effect observed at both methyl and carboxyl carbons of acetate. 9. Pyruvate synthase is distinct from pyruvate dehydrogenase, for which the isotope effect at C-3 is *ca.* 9‰ (Melzer and Schmidt, 1987). Both enzymes use thiamine pyrophosphate as a cofactor. 10. Preuß *et al.* (1989) identify PEP carboxykinase as important in completion of the acetyl-CoA pathway in *Acetobacterium woodii*. 11. Preuß *et al.* (1989). 12. van der Meer *et al.* (2001b). 13. Although the immediate C-fixing processes yield malonyl- and methylmalonyl-CoA, the net product of the 3-hydroxypropionate cycle is glyoxylate, a C<sub>2</sub> molecule. The processes by which glyoxylate is assimilated and converted to biomass are not known (Strauss and Fuchs, 1993).

drude donor or reductant. A typical reaction is shown below. Note that NADPH + H<sup>+</sup> is equivalent to NADP<sup>+</sup> + H<sub>2</sub>.



The isotopic composition of the H<sup>+</sup> transferred from NADPH to biosynthetic substrates must be one of the most important factors controlling the hydrogen-isotopic

composition of organic matter.

For contrast and completeness, NAD<sup>+</sup> and NADH should be introduced here. NAD<sup>+</sup> is the oxidized form of nicotinamide adenine dinucleotide. It is structurally identical to NADP<sup>+</sup> except that it lacks a phosphate group at a key point. Order and control are brought to biochemical oxidations and reductions by this seemingly trivial distinction. NAD<sup>+</sup> is generally an oxidant. NADPH is generally a reductant. Each is present within a cell at only microscopic



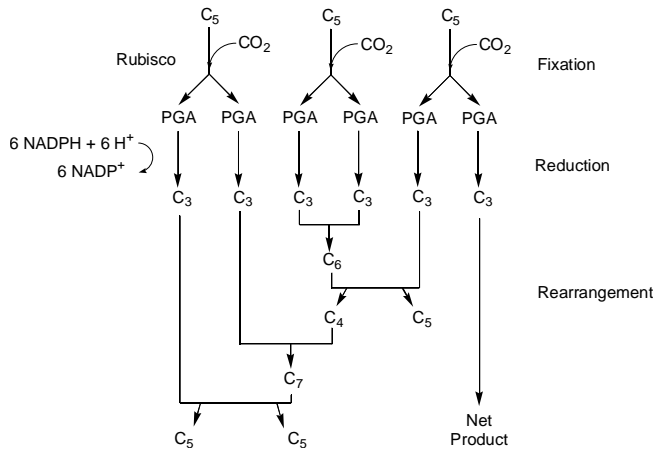
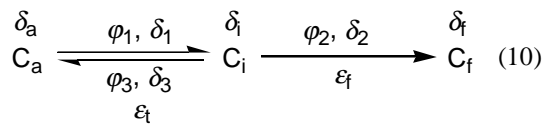


**Figure 8.** A schematic view of the flow of carbon in the Calvin Cycle. Subscripted Cs represent carbohydrates for which the net oxidation number for carbon is zero. PGA represents 3-phosphoglyceric acid. Six moles of NADPH + H<sup>+</sup> are required to provide the 12 electrons required to reduce three moles of carbon initially in the form of CO<sub>2</sub> to the level of carbohydrate. Energy provided by the hydrolysis of ATP (not shown) is required to drive the overall process.



where  $C_a$ ,  $C_i$ , and  $C_f$  represent respectively the ambient CO<sub>2</sub> (an infinite, stirred reservoir), the CO<sub>2</sub> inside the cell (at the active site of rubisco), and the fixed carbon (the carboxyl groups in PGA that derive from CO<sub>2</sub>). The isotope effects  $\varepsilon_i$  and  $\varepsilon_f$  are respectively those associated with mass transport of CO<sub>2</sub> to and from the reaction site and with the fixation of CO<sub>2</sub>. At steady state, mass balance must prevail at the  $C_i$  branch point. By analogy with equation 4, we can write

$$\delta_i = f_2 \delta_2 + (1 - f_2) \delta_3 \quad (11)$$

where  $f_2 \equiv \varphi_2 / (\varphi_2 + \varphi_3)$ . Substituting  $\delta_i = \delta_a - \varepsilon_i$ ,  $\delta_2 = \delta_i - \varepsilon_f$ , and  $\delta_3 = \delta_i - \varepsilon_i$  yields an equation relating  $\delta_a$ ,  $f_2$ , the isotope effects, and  $\delta_i$ . Substitution of  $\delta_i = \delta_f + \varepsilon_f$  allows elimination of  $\delta_i$  and provides the result

$$\varepsilon_p = \delta_a - \delta_f = \varepsilon_f - f_2(\varepsilon_f - \varepsilon_i) \quad (12)$$

where  $\varepsilon_p$  is the overall fractionation between  $C_a$  and  $C_f$ .

The form of equation 12 differs from that of standard presentations. In considerations of emergent plants,  $f_2$  is usually cast in terms of  $p_i$  and  $p_a$ , the internal and ambient partial pressures of CO<sub>2</sub> (Farquhar *et al.*, 1989). For aquatic plants, various substitutions allow  $f_2$  to be expressed in terms of  $c_e$ , the concentration of dissolved CO<sub>2</sub> in the water in which the plant is growing (Laws *et al.*, 1995; Popp *et al.*, 1998b). In all cases, however, the result is equivalent to that called for by equation 12. As  $f_2 \rightarrow 0$  (as  $p_i$  approaches  $p_a$  or as concentrations of dissolved CO<sub>2</sub> become so high that only the enzymatic reaction limits the rate of fixation),  $\varepsilon_p \rightarrow \varepsilon_f$ . Alternatively, if  $f_2 \rightarrow 1$ , indicating that near-

ly every molecule of CO<sub>2</sub> that enters the plant is fixed, then  $\varepsilon_p \rightarrow \varepsilon_i$ . These extremes can also be summarized phenomenologically: if the rate of fixation is limited only by the enzymatic reaction, then the resulting free exchange of CO<sub>2</sub> between the cell and its surroundings allows maximal expression of the enzymatic isotope effect. On the other hand, if every molecule of CO<sub>2</sub> that enters the plant is fixed, then the only isotope effect visible will be that of mass transport.

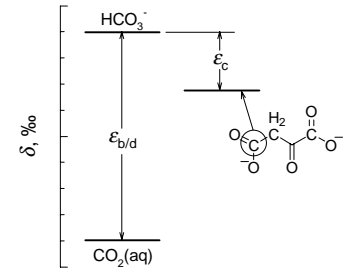
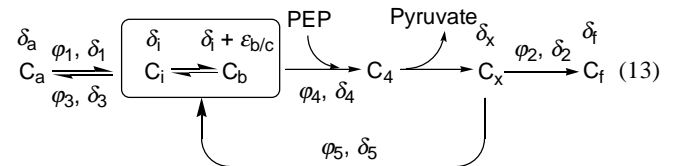


**Figure 9.** Diagram summarizing the isotopic relationships between dissolved CO<sub>2</sub>, bicarbonate, and the carbon added to phosphoenolpyruvate in order to produce C-4 in oxaloacetate.

In the context established by equation 10,  $\varepsilon_f$  is the net isotope effect associated with the fixation of inorganic carbon. As noted in Table 2, for C<sub>3</sub> plants this includes not only the rubisco-catalyzed carboxylation of RuBP but also the fixation of bicarbonate by PEP carboxylase. The latter process has a much smaller isotope effect *and* it utilizes a carbon source that is enriched in <sup>13</sup>C relative to dissolved CO<sub>2</sub>. These factors are indicated schematically in Figure 9, which shows that carbon fixed by PEP carboxylase will be enriched in <sup>13</sup>C relative to dissolved CO<sub>2</sub>. As a result of such phenomena,  $\varepsilon_f$  is smaller than the  $\varepsilon$  listed in Table 2 for rubisco itself. The difference depends on the amount of C fixed by PEP carboxylase. For land plants, Farquhar *et al.* (1989) estimate  $\varepsilon_f = 27\%$ . For unicellular, eukaryotic phytoplankton, Popp *et al.* (1998b) find  $\varepsilon_f = 25\%$ . The difference indicates either that fixation of C by PEP carboxylase is more important in algae or that the rubisco in those organisms has a slightly lower isotope effect than the enzyme present in higher plants. Values of  $\varepsilon_i$  are 4.4‰ for emergent plants in which the rate-determining transport of CO<sub>2</sub> occurs in air and 0.8‰ for plants that grow under water (0.7‰, O'Leary, 1984; 0.87‰, Jähne *et al.*, 1987). Rubisco exists in multiple forms with differing isotope effects (Robinson and Cavanaugh, 1995). Values of  $\varepsilon_{\text{rubisco}}$  are 29‰ for higher plants (Roeske and O'Leary, 1984), and apparently somewhat lower for most phytoplankton and bacteria (Roeske and O'Leary, 1985; Guy *et al.*, 1993; Robinson and Cavanaugh, 1995; Popp *et al.*, 1998b).

#### Isotopic fractionations, C<sub>4</sub> pathway

The reaction network for a C<sub>4</sub> plant is shown below:



Terms are defined in parallel with those in reaction 10, with the addition of  $C_b$ ,  $C_4$ , and  $C_x$  which indicate respectively

bicarbonate in equilibrium with  $\text{CO}_2$  in mesophyll cells, C added to phosphoenolpyruvate (PEP) to produce malate and oxaloacetate, and  $\text{CO}_2$  released by decarboxylation of oxaloacetate. Leakage of  $\text{CO}_2$  from the site of decarboxylation is represented by  $\varphi_5$ . Taking this into account is a key factor if we are to understand variations in fractionation associated with the  $\text{C}_4$  pathway. Two branch points appear in this network. For carbon in mesophyll cells we require

$$\varphi_1 \delta_1 + \varphi_5 \delta_5 = \varphi_4 \delta_4 + \varphi_3 \delta_3 \quad (14)$$

and, for carbon released by decarboxylation of oxaloacetate:

$$\varphi_4 \delta_4 = \varphi_5 \delta_5 + \varphi_2 \delta_2 \quad (15)$$

Defining a leakage parameter,  $L \equiv \varphi_5 / \varphi_4$ , we obtain

$$\delta_4 = L(\delta_5 - \delta_2) + \delta_2 \quad (16)$$

Relating the isotopic compositions of the specified fluxes of carbon to those of the various carbon pools, we can write  $\delta_1 = \delta_a - \varepsilon_{\text{ta}}$ ,  $\delta_3 = \delta_1 - \varepsilon_{\text{ta}}$ ,  $\delta_4 = \delta_1 + \varepsilon_{\text{b/d}} - \varepsilon_c$ ,  $\delta_2 = \delta_s - \varepsilon_f$ , and  $\delta_5 = \delta_x - \varepsilon_{\text{tw}}$ , where  $\varepsilon_{\text{ta}}$  and  $\varepsilon_{\text{tw}}$  are respectively the isotope effects associated with mass transport of  $\text{CO}_2$  in air and in water (as specified above, 4.4 and 0.8‰, respectively),  $\varepsilon_{\text{b/d}}$  is the equilibrium isotope effect relating bicarbonate and dissolved  $\text{CO}_2$  (Mook *et al.*, 1974), and  $\varepsilon_c$  is the isotope effect associated with fixation of bicarbonate by phosphoenolpyruvate carboxylase (O'Leary *et al.*, 1981; here we use a compromise value of 2.2‰ implied by O'Leary, 1981).

Using the relationships specified, our task is to rearrange and combine equations 14-16 in order to produce an expression for  $\varepsilon_{\text{p4}}$  ( $\approx \delta_a - \delta_f = \delta_a - \delta_2$ ), the net isotopic fractionation associated with the  $\text{C}_4$  pathway. Using  $\delta_5 - \delta_2 = \varepsilon_f - \varepsilon_{\text{tw}}$ , equation 16 can be rewritten as  $\delta_4 = L(\varepsilon_f - \varepsilon_{\text{tw}}) + \delta_2$ . Substituting for  $\delta_4$  yields an expression incorporating  $\varepsilon_c$ :

$$\delta_1 + \varepsilon_{\text{b/d}} - \varepsilon_c = L(\varepsilon_f - \varepsilon_{\text{tw}}) + \delta_2 \quad (17)$$

Terms relating to the mass balance at  $\text{C}_i$  must be incorporated and  $\delta_1$ , which can't be measured, must be eliminated. To accomplish these steps, we substitute  $\delta_1 = \delta_3 + \varepsilon_{\text{ta}}$ , replacing  $\delta_3$  by an expression obtained by rearranging equation 14. The result is

$$\varphi_1 \delta_1 + \varphi_5 \delta_5 - \varphi_4 \delta_4 + \varphi_3 \varepsilon_{\text{ta}} + \varphi_3 (\varepsilon_{\text{ta}} + \varepsilon_{\text{b/d}} - \varepsilon_c) = \varphi_3 L (\varepsilon_f - \varepsilon_{\text{tw}}) + \varphi_3 \delta_2 \quad (18)$$

Division by  $\varphi_1$  yields important terms with the coefficient  $\varphi_3 / \varphi_1$ , which is equal to  $1 - f_2$ . A final substitution for  $\delta_5$  based on rearrangement of equation 15 yields

$$\delta_a - \delta_2 = \varepsilon_{\text{p4}} = \varepsilon_{\text{ta}} + [\varepsilon_c - \varepsilon_{\text{b/d}} + L(\varepsilon_f - \varepsilon_{\text{tw}}) - \varepsilon_{\text{ta}}](1 - f_2) \quad (19)$$

This equation relates  $\varepsilon_{\text{p4}}$  to the minimum number of controlling variables, specifically the isotope effects and the branching ratios ( $L, f_2$ ) within the reaction network. Earlier, Farquhar (1983) presented a physiologically based derivation of an expression for  $\varepsilon_{\text{p4}}$ . Equation 19 is precisely equivalent except for the coefficient for  $L$ . The earlier derivation adopted  $\varepsilon_{\text{tw}} \approx 0$  and thus yielded  $L\varepsilon_f$  rather than  $L(\varepsilon_f - \varepsilon_{\text{tw}})$ . Expressed in terms of the internal and ambient

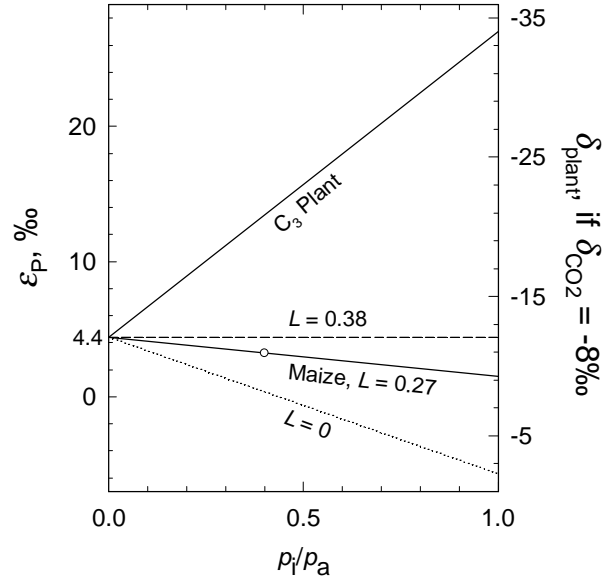


**Figure 10.** Overall isotopic fractionation (essentially the difference between  $\text{CO}_2$  and biomass) as a function of  $p_i/p_a$ , the ratio of partial pressures of  $\text{CO}_2$  inside and outside C-fixing cells. The scale on the right-hand axis is inverted and shows  $\delta_{\text{biomass}}$  for plants using  $\text{CO}_2$  with  $\delta = -8\text{‰}$ . The solid lines represent  $\text{C}_3$  plants and maize, a representative  $\text{C}_4$  plant, with the point indicating its typical value of  $p_i/p_a$  (Marino and McElroy, 1991). The horizontal dashed line shows that  $\varepsilon_p$  is independent of  $p_i/p_a$  when  $L$ , the leakiness coefficient for bundle-sheath cells in a  $\text{C}_4$  plant, is 0.38 (see equations 13-19 and accompanying discussion). The dotted line represents a (hypothetical) plant with gas-tight bundle-sheath cells and indicates that the biomass of such a plant could be enriched in  $^{13}\text{C}$  relative to  $\text{CO}_2$  for  $p_i/p_a > 0.45$ .

partial pressures of  $\text{CO}_2$ ,  $1 - f_2 = p_i/p_a$ .

Two important aspects of the carbon isotopic fractionation imposed by the  $\text{C}_4$  pathway are summarized graphically in Figures 9 and 10. The first schematically indicates the carbon-isotopic relationships between dissolved  $\text{CO}_2$ , bicarbonate, and the carbon that is added to phosphoenolpyruvate in the reaction catalyzed by phosphoenolpyruvate carboxylase. It shows that, because the kinetic isotope effect associated with PEP carboxylase is smaller than the equilibrium isotope effect between dissolved  $\text{CO}_2$  and bicarbonate, the fixed carbon is enriched in  $^{13}\text{C}$  relative to that in the dissolved  $\text{CO}_2$ . As result, the  $\text{CO}_2$  subsequently made available to rubisco in CAM and  $\text{C}_4$  plants is enriched in  $^{13}\text{C}$  relative to atmospheric  $\text{CO}_2$ . If that carbon were fixed with perfect efficiency, the biomass of the plant would be enriched in  $^{13}\text{C}$  relative to  $\text{CO}_2$  from the atmosphere –  $\varepsilon_{\text{p4}}$  would be negative, indicating an inverse fractionation.

Values of  $\delta_1$  and  $\delta_x$  (see reaction 13) are, however, influenced strongly by the branching ratios at the  $\text{C}_i$  and  $\text{C}_x$  branch points. The first pertains to exchange of  $\text{CO}_2$  between the atmosphere and the plant. As long as the

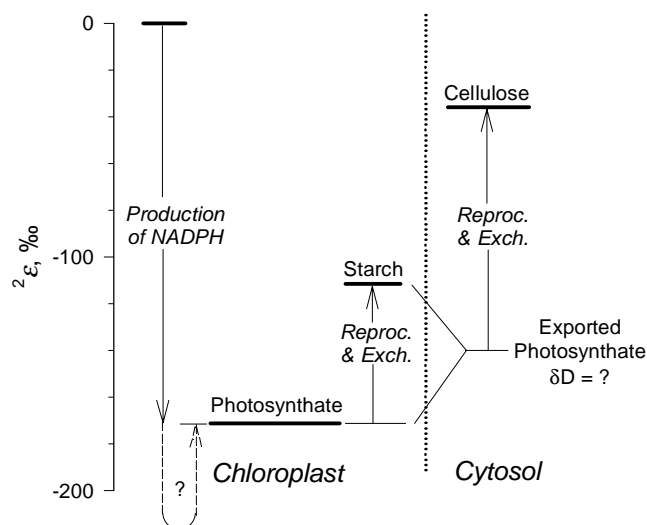


**Figure 11.** Relationships between the hydrogen isotopic compositions of initial photosynthate and related products and of water available within plant cells. The uncertainty indicated on the pathway between water and photosynthate reflects the possibility of offsetting fractionations in the production of NADPH and the subsequent transfer of H<sup>+</sup> to photosynthate.

partial pressure of CO<sub>2</sub> in the interior air spaces of the leaf is not zero, CO<sub>2</sub> will be diffusing out of the plant as well as into it. The second pertains to leakage of CO<sub>2</sub> away from the site at which oxaloacetate is decarboxylated. Depending on whether that leakage is minimal or extreme, the isotope effect associated with rubisco will be expressed to a lesser or greater degree at the C<sub>x</sub> branch point. Net fractionations are plotted as a function of  $L$  and  $p_i/p_a$  in Figure 10. For all cases,  $p_i/p_a = 0$  corresponds to a situation in which carbon fixation is limited entirely by the transport of CO<sub>2</sub> into the plant. Accordingly,  $p_i/p_a = 0$  requires  $\epsilon_{p_4} = \epsilon_{ta} = 4.4\text{‰}$ , independent of  $L$ . If no CO<sub>2</sub> leaked away from the site of decarboxylation of oxaloacetate but, at the same time, the plant was very freely exchanging CO<sub>2</sub> with the atmosphere – an implausible combination of circumstances corresponding to  $p_i/p_a \approx 1$  and  $L = 0$  – maximal inverse fractionation would result, with the fixed carbon being enriched in <sup>13</sup>C relative to atmospheric CO<sub>2</sub> by 5.7‰ (for  $\epsilon_{v/d} = 7.9\text{‰}$  at 25°C). In contrast to these extremes, maize, a representative C<sub>4</sub> plant, typically has  $L = 0.27$  and  $p_i/p_a = 0.4$  (Marino and McElroy, 1991). Consistent with these values, measurements of the fractionation between atmospheric CO<sub>2</sub> and cellulose from corn kernels consistently yielded  $\epsilon_{p_4} = 3.28\text{‰}$  (Marino and McElroy, 1991). Given the weak dependence of  $\epsilon_{p_4}$  on  $p_i/p_a$  (a hypothetical C<sub>4</sub> plant with  $L = 0.38$  would yield  $\epsilon_{p_4}$  independent of  $p_i/p_a$ ), Marino and McElroy (1991) proposed that C<sub>4</sub>-plant debris could provide a record of the isotopic composition of atmospheric CO<sub>2</sub>. For CAM plants, which lack the specialized, bundle-sheath cells found in C<sub>4</sub> plants, values of  $L$  are significantly higher and, as a result, isotopic depletions are significantly greater.

Table 3. Hydrogen isotopic fractionations measured in aquatic plants

	$\epsilon_{C/w}^a$	$\epsilon_{H/w}^b$	$n^c$	Reference
Cyanobacteria		$-198 \pm 17$	4	Estep and Hoering, 1980
Macrophytes		$-152 \pm 27$	16	Estep and Hoering, 1980
Red algae	$-45 \pm 31$	$-139 \pm 25$	13	Sternberg <i>et al.</i> , 1986
Brown algae	$-42 \pm 42$	$-178 \pm 11$	21	Sternberg <i>et al.</i> , 1986
Green algae	$-141 \pm 56$	$-132 \pm 18$	6	Sternberg <i>et al.</i> , 1986
Macrophytes	$1 \pm 40$	$-125 \pm 20$	21	Sternberg, 1988

<sup>a</sup>  $\equiv 1000[(\delta_{\text{Cellulose}} + 1000)/(\delta_{\text{water}} + 1000) - 1]$  (non-exchangeable H only)

<sup>b</sup>  $\equiv 1000[(\delta_{\text{Lipids}} + 1000)/(\delta_{\text{water}} + 1000) - 1]$

<sup>c</sup> number of specimens; indicated uncertainties are standard deviations of populations

<sup>d</sup> Tabulated entry refers to saponifiable lipids. Fractionation for saponifiable lipids in the same samples =  $-232 \pm 32\text{‰}$ .

### Hydrogen isotopes in carbohydrates

Hydrogen is introduced by the reduction of PGA, with NADPH serving as the hydride donor (*cf.* reaction 7). As shown in Figure 8, the fixed carbon and its accompanying, “non-exchangeable” hydrogen (the H directly bonded to C) are then shuffled among C<sub>3</sub>, C<sub>4</sub>, C<sub>5</sub>, C<sub>6</sub>, and C<sub>7</sub> sugars. The net effects are regeneration of ribulose bisphosphate and repackaging of fixed C and H into trioses (glyceraldehyde, dihydroxyacetone) and hexoses (fructose, glucose). These products can be used in biosynthesis, exported to the cytosol, or stored within the chloroplast as starch. The inventory of C-bound H remains constant within the Calvin Cycle. Isotopic fractionations can, therefore, only affect the distribution of D among positions, not the overall  $\delta$ value. The hydrogen can, however, be partly exchanged with H<sub>2</sub>O in the course of the numerous rearrangements within the Calvin Cycle. Yakir and DeNiro (1990) have reviewed earlier work and have experimentally isolated the production of photosynthate well enough to estimate  $\epsilon_{p/w} = -171\text{‰}$ , where P designates photosynthate and w the water used by the plant. That isotopic relationship between water and photosynthate is indicated schematically at the left of Figure 11. The sketch includes some broken lines and a question mark to indicate that the fractionation might represent the net of two or more processes. These could include the transfer of H from H<sub>2</sub>O to NADP<sup>+</sup>, possibly favoring H that was strongly depleted in D (Luo *et al.*, 1991); the transfer of H from NADPH to PGA; and subsequent exchanges of C-bound H with H<sub>2</sub>O, a process which is known to favor partitioning of D into the carbohydrate ( $1.00 \leq K \leq 1.18$ ; Cleland *et al.*, 1977).

There are ample opportunities for further hydrogen-isotopic fractionations. These have been well studied for the specific case of the non-exchangeable H in cellulose. As demonstrated by the examples cited in Table 3, they attenuate the fractionation imposed during the initial production of photosynthate. None of the values of  $\epsilon_{C/w}$  is as large as 171‰. Yakir (1992) has reviewed evidence show-

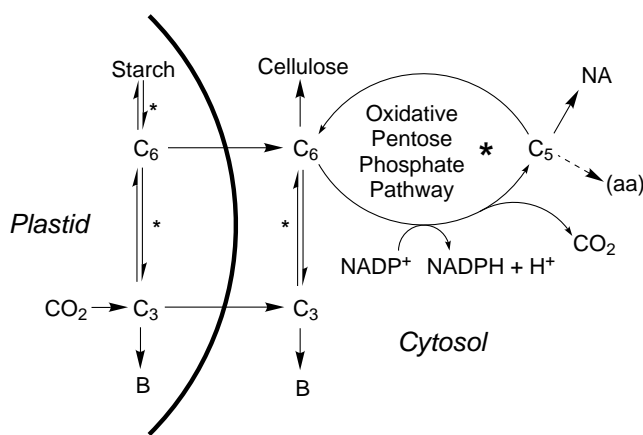


**Figure 12.** The flow of H from initial photosynthate ( $C_3$  within the chloroplast) to stored carbohydrates and to cytosolic NADPH. Asterisks mark processes in which exchange of C-bound H with water is likely. B, biomass; NA, nucleic acids; (aa), minor contribution to amino acids.

ing that this apparent recovery of D is associated with the “heterotrophic processing” of photosynthate. This occurs when carbohydrates are degraded to yield carbon, energy, and reducing power for the biosynthesis of lipids and proteins. The oxidative pentose phosphate pathway is particularly important in this regard. As shown in Figure 12, it involves the partial oxidation of  $C_6$  sugars and serves as a source for NADPH outside the chloroplast (in green algae, it also operates within the chloroplast; Falkowski and Raven, 1997, p. 241). The  $C_5$  products, pentoses, are repackaged to form new hexoses which can be condensed to form cellulose. Up to 50% of the C-bound H exchanges with water during this repackaging (Yakir and DeNiro, 1990). To examine the effects of the reprocessing of carbohydrates in the cytoplasm, Luo and Sternberg (1991) compared the hydrogen-isotopic composition of plastidic starch with that of cellulose. As noted in Figure 11, the cellulose – built from exchange-affected cytosolic glucose – was consistently enriched in D, the average difference for five CAM plants and six  $C_3$  plants being about 80%.

#### Intramolecular carbon-isotopic order in carbohydrates

The carbon-isotopic fractionations described thus far have pertained to fixed carbon entering the Calvin Cycle. The extensive transfers of carbon within that cycle might be expected to act as an isotopic mixer, so that the distribution of  $^{13}C$  within carbohydrates from photosynthate would be uniform. To examine this hypothesis, Rossmann *et al.* (1991) used chemical degradations and microbial fermentations to produce  $CO_2$  from each of the six carbon positions within glucose. One sample of glucose was from corn starch (maize, a  $C_4$  plant) and the other was from sucrose from sugar beets ( $C_3$ ). Both samples represented cytoplasmic, storage forms of carbohydrate and both yielded closely similar results. Relative to the average for the molecule, positions C-3 and C-4 were enriched in  $^{13}C$  by 2 and 5%, respectively, and position C-6 was depleted by 5%. The

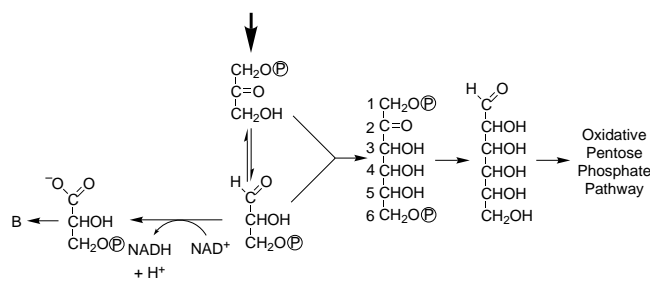


**Figure 13.** Flow of carbon from dihydroxyacetone phosphate to phosphoglyceraldehyde (and, with oxidation, to 3-phosphoglyceric acid and biomass) and to  $C_6$  sugars. As shown, fructose-1,6-bisphosphate can be formed by combining dihydroxyacetone phosphate and phosphoglyceraldehyde. The further sugar shown has the structure of glucose (stereochemistry not shown). Carbon positions in such aldohexoses are numbered 1-6, starting with the aldehydic carbon. The processes indicated are possibly related to the intramolecular distribution of  $^{13}C$  in glucose observed by Rossmann *et al.* (1991).

precision of the analyses was such that the apparent imbalance (more enrichment than depletion) is not significant, but the consistency between plants and between the chemical and fermentative degradations is impressive. The evidence for isotopic inhomogeneity is substantial.

The relevant reaction network is shown in Figure 13. The input to the system is dihydroxyacetone phosphate, exported from the chloroplast. In the cytosol, its equilibration with glyceraldehyde-3-phosphate is catalyzed by triose-phosphate isomerase. As the first step in respiratory metabolism or in biosyntheses requiring  $C_2$  units, a portion of the glyceraldehyde-3-phosphate is dehydrogenated to yield PGA. Rossmann *et al.* (1991) suggest that an isotope effect associated with this reaction could lead to enrichment of  $^{13}C$  at the aldehyde carbon in glyceraldehyde-3-phosphate and that, by action of the triose phosphate isomerase, the enrichment could propagate to the free-alcohol carbon in dihydroxyacetone phosphate. Since these carbons flow to positions C-4 and C-3, respectively, in glucose, the mechanism provides a good explanation for the isotopic enrichment at those positions, even accounting for the greater enrichment at C-4. The depletion of  $^{13}C$  at C-6 is unexplained. Rossmann *et al.* (1991) speculate that it arises because C-6 is sheltered from all of the bond-making and -breaking in the oxidative pentose phosphate pathway, which provides an independent means of affecting isotopic compositions within glucose. This might be the beginning of a correct explanation, but C-5 is also relatively sheltered and seems not to be isotopically unusual.

#### Isotopic Compositions of Amino Acids

Amino acids are unique in that the first report of their isotopic compositions also provided intramolecular analyses (*n. b.*, intramolecular = position-specific). In fact, the paper by Abelson and Hoering (1961) introduced the concept of intramolecular isotopic order and thus established a new basis for understanding the isotopic compositions of

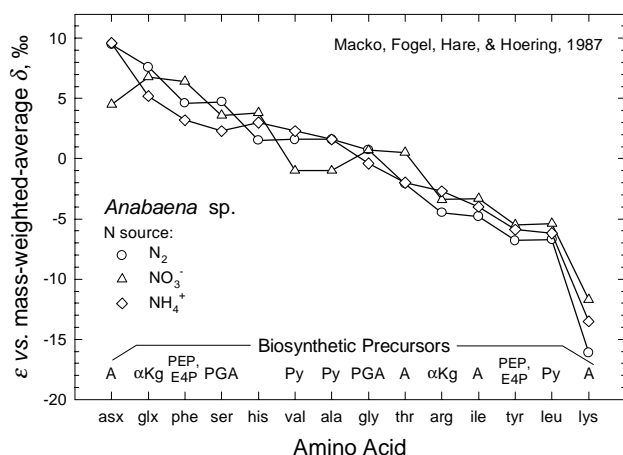
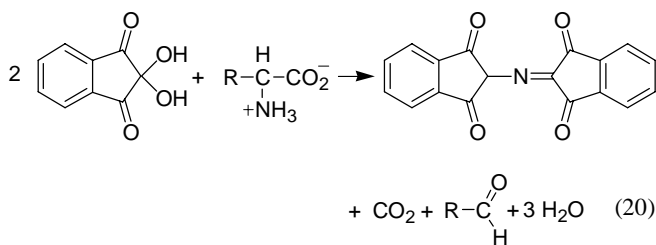


**Figure 14.** Carbon-isotopic compositions of individual amino acids synthesized by the cyanobacteria *Anabaena* sp. Strain IF ( $N_2$ -fixing and  $NO_3^-$ -utilizing cultures) and Strain CA ( $NH_4^+$ -utilizing culture). Abundances of  $^{13}C$  are expressed in terms of  $\epsilon$ , the fractionation relative to the mass-weighted isotopic composition of all of the amino acids analyzed from each culture (Macko *et al.*, 1987). The abbreviations specified in Table 1 are used to designate the amino acids. Abbreviations above the horizontal axis specify biosynthetic families: A, aspartic acid;  $\alpha$ Kg,  $\alpha$ -ketoglutarate; PEP+E4P, phosphoenolpyruvate + erythrose-4-phosphate; PGA, phosphoglyceric acid; and Py, pyruvate. Histidine (his) is synthesized by a unique pathway. Lysine (lys) is a member of the aspartic-acid family except in *Euglena* and fungi, where it is a member of the  $\alpha$ -ketoglutarate family.

organic compounds. The breakthrough resulted in part from the development of ion-exchange-chromatographic techniques for the separation of amino acids. This high-resolution, liquid chromatographic technique provided quantities that were large enough for isotopic analyses using the techniques available in 1960. In conventional analyses, amino acids were detected by mixing the column effluent stream with a solution of ninhydrin. The resulting reaction, essentially quantitative (Moore and Stein, 1951), produces a strongly colored product that can be detected spectrophotometrically. In their preparative separations, Abelson and Hoering spiked initial hydrolysates with traces of radiocarbon-labeled amino acids and followed them through the separations. Peaks were collected and aliquots were treated with ninhydrin:



As shown in the equation above,  $\text{CO}_2$  is produced from the carboxyl group of the amino acid. Because the reaction is essentially quantitative, the isotopic composition of the  $\text{CO}_2$  specifically reflects the abundance of  $^{13}C$  in the carboxyl group.

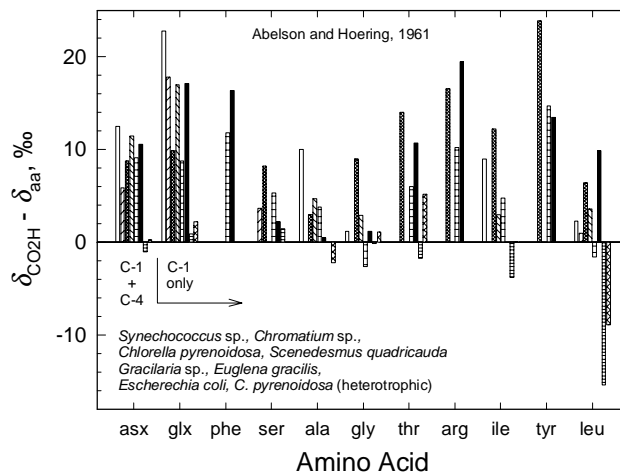


**Figure 15.** Enrichments (and rare depletions) of  $^{13}C$  in carboxyl groups of amino acids as measured by Abelson and Hoering (1961). Enrichments and depletions are expressed relative to the overall average for each amino acid, *not* relative to the non-carboxyl carbon. Within each cluster, the bars refer in left-to-right sequence to the organisms listed (*Synechococcus* sp. is the present name of the organism identified as *Anacystis nidulans* in the original publications), with the last two representing heterotrophic cultures. As noted, the analytical procedure utilized produced  $\text{CO}_2$  from both carboxyl groups in asp but only from the C-1 carboxyl group in glu.

#### $^{13}C$ in individual amino acids

More recent results from the Geophysical Laboratory – the site of Abelson and Hoering's (1961) seminal investigations – provide the best starting point for a consideration of the carbon-isotopic fractionations associated with the biosyntheses of amino acids. These later results, summarized graphically in Figure 14, come from a by-then-highly-experienced team of isotopic and amino-acid analysts (Macko *et al.*, 1987). They relate to the simplest possible autotrophic system, a cyanobacterium grown under optimal conditions with continuous illumination and harvested in late log phase. Under these conditions, complications arising from the reversible carbon flows generally characteristic of amino acid biosyntheses must be minimized.

The intramolecular isotopic distributions reported by Abelson and Hoering (1961), though less precise and based on less carefully cultured organisms, provide further information. The results are summarized graphically in Figure 15. Positive vertical bars reflect enrichment of  $^{13}C$  in the carboxyl group relative to the molecule as a whole. Even assigning an uncertainty of  $\pm 3\%$  to each result, a few observations appear robust: (i) carboxyl groups of amino acids from autotrophs are generally enriched in  $^{13}C$  relative to the rest of the molecule, with particularly strong enrichments in asx and glx, in the aromatic amino acids (phe and tyr), and in arg; and (ii) intramolecular contrasts in amino acids produced by organisms growing heterotrophically are generally smaller, with the notable exception of carboxyl groups in leu, which are strongly depleted in  $^{13}C$  relative to the rest of the molecule.

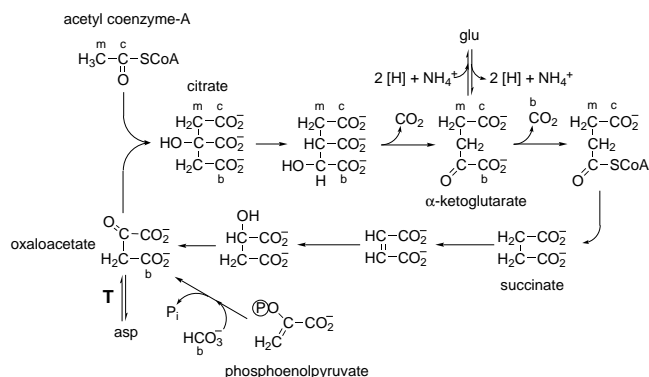


**Figure 16.** A schematic view of the flow of carbon within the tricarboxylic acid cycle. The labels *m*, *c*, and *b* designate respectively carbon from the methyl and carboxyl positions of acetyl-CoA and from bicarbonate used to produce oxaloacetate from phosphoenolpyruvate. Inputs and outputs of water, of redox cofactors ( $\text{NAD}^+$ , *etc.*), and of coenzymes (CoASH) have been omitted in order to focus on the carbon skeletons. The amination of  $\alpha$ -ketoglutarate in order to produce glu is the principal means of importing N for use in the amino-acid pool. The process involves multiple steps, including a reduction (indicated by addition of  $[\text{H}]$ ) and is represented here only schematically. The boldface T indicates transamination, an example of which is shown in equation 21. The circled P represents a phosphate group,  $\text{PO}_3^{2-}$ .  $\text{P}_i$  represents inorganic phosphate,  $\text{HPO}_4^{2-}$ .

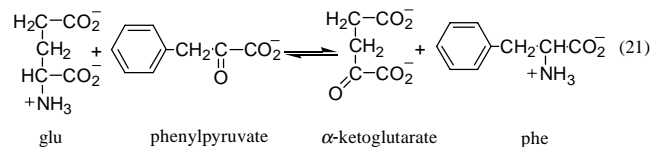
Additional intramolecular analyses of aspartate have been reported by Melzer and O'Leary (1987, 1991). These authors examined aspartate produced by  $\text{C}_3$  higher plants and showed that C-4, the carboxyl group not involved in peptide bonding, is commonly enriched in  $^{13}\text{C}$  by 10-12% relative to the rest of the molecule. The enrichment at C-4 in aspartate from  $\text{C}_4$  plants is about half as large.

The amino acids are commonly divided into families based on their biosynthetic origins. These are indicated above the horizontal axis in Figure 14. The abbreviations and gaps are explained in the caption and the pathways are described below. The zero point of the  $\epsilon$  scale in Figure 14 is set by the mass-weighted average isotopic composition of all of the amino acids analyzed. That point is probably about 1‰ above the biomass-average  $\delta$  (see eq. 5 and related discussion). With allowances for respiratory losses of fixed carbon, the isotopic composition of photosynthate – the  $\delta$  value of  $\text{C}_3$  units being supplied to biosynthetic processes – is probably another 0.5‰ lower, near -1.5‰ on the  $\epsilon$  scale defined in Figure 14. By this measure, thr is practically unfractionated relative to photosynthate and val, ala, and gly are only slightly enriched in  $^{13}\text{C}$ . The left-to-right ordering of the amino acids was arranged to yield declining abundances of  $^{13}\text{C}$ . Very clearly, it has *not* separated the amino acids into their biosynthetic families. Representatives of the aspartic acid family, for example, are spread from one end of the axis to the other. Do such depletions represent fractionations caused by successive isotope effects or must other explanations be sought?

The tricarboxylic acid cycle (TCA cycle) provides a

logical starting point. Relationships between carbon skeletons in that cycle are shown in Figure 16. The TCA cycle is normally thought of as the central carbon-processing facility of respiratory metabolism. As shown, acetyl groups are transferred from coenzyme A to oxaloacetate in order to produce citrate. The citrate is oxidatively decarboxylated to yield  $\alpha$ -ketoglutarate which is in turn oxidatively decarboxylated to yield succinate. The succinate is further oxidized to yield oxaloacetate, thus regenerating the reactant needed for the next turn of the cycle. In effect, acetate is burned to yield  $\text{CO}_2$ . The oxygen required comes from  $\text{H}_2\text{O}$ . The redox budget is balanced by removal of  $\text{H}_2$  (in the form of  $\text{NADH} + \text{H}^+$ , not shown in Figure 16). A separate system (the “electron-transport chain”) uses an inorganic electron acceptor ( $\text{O}_2$ ,  $\text{NO}_3^-$ ,  $\text{SO}_4^{2-}$ , among others) to oxidize the  $\text{H}_2$  and conserves the energy produced by the oxidation of the acetate. Quite apart from its role in oxidative metabolism, the TCA cycle is important to amino-acid biosynthesis because, by producing oxaloacetate and  $\alpha$ -ketoglutarate, it provides the carbon skeletons for aspartic and glutamic acids (notably the amino acids most strongly enriched in  $^{13}\text{C}$ , see Fig. 14).

The key step in amino-acid biosynthesis is production of the carbon skeleton rather than the amino acid itself. Given the carbon skeleton, the process is completed by transamination. An example is shown in reaction 21.



In this case, the availability of phenylpyruvic acid allows production of phenylalanine. As shown, amino groups are generally provided by glutamic acid. A special system exists for the production of glutamate from  $\alpha$ -ketoglutarate +  $\text{NH}_4^+$ . With this basic information we can now consider specific biosyntheses.

The aspartic-acid family can be considered first. The relationship of aspartic acid to oxaloacetate (OAA) and thus to the TCA cycle creates a problem, particularly for growing photoautotrophs. Aspartic acid is a very common amino acid. Relatively large quantities are required for the synthesis of proteins. If all the OAA is used to make aspartate, the TCA cycle will be shut down because citrate cannot be synthesized. An alternate source of OAA is therefore required. As shown in Figure 16, this is provided by the carboxylation of phosphoenolpyruvate (PEP), which can be formed directly from the products of  $\text{C}_3$  photosynthesis. The resulting isotopic relationships are indicated schematically in Figure 17, which considers a representative  $\text{C}_3$  plant with  $\delta_a = -8$  and  $\delta_f = -25$ ‰. The internal  $\text{CO}_2$  will have  $\delta_i = 2$ ‰ (from  $\delta_i = \delta_f + \epsilon_p$ , see eq. 11 and accompanying discussion) and the bicarbonate available to PEP carboxylase will be further enriched as a result of the isotope effect associated with the  $\text{CO}_2$ -equilibrium. The car-

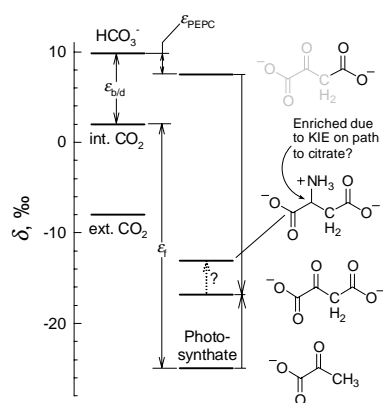


**Figure 17.** Diagram summarizing isotopic relationships between inorganic carbon pools and carbon in photosynthate and  $C_4$  carbon skeletons.  $\epsilon_{b/d}$  is the equilibrium isotopic fractionation between dissolved  $CO_2$  and bicarbonate (Mook *et al.*, 1974).  $\epsilon_f$  is the isotope effect associated with carbon fixation. The estimate of  $\delta$  for internal  $CO_2$  is based on  $\delta_{\text{photosynthate}} = -25\text{‰}$  and  $\epsilon_f = 27\text{‰}$ .  $\epsilon_{\text{PEPC}}$  is the isotope effect associated with phosphoenolpyruvate carboxylase (O'Leary *et al.*, 1982). The carbon pools represented in the right-hand column are, from top to bottom, the carbon added by the carboxylation of phosphoenolpyruvate, the total carbon in aspartic acid and in oxaloacetate, and the total carbon in pyruvate.

enriched by 32‰ relative to the other three carbon atoms in the molecule, assuming that their isotopic composition does not differ from that of photosynthate. The average  $\delta$  for the four-carbon molecule is thus pulled up by 8‰. This is already in good agreement with the enrichments in asp relative to photosynthate (roughly represented in Fig. 14 by gly or thr). Further enrichment is possible if there is an isotope effect at C-2 in OAA during the formation of citrate. At steady state, such an effect would lead to a pile-up of  $^{13}C$  at C-2 in the OAA pool. The 10-12‰ enrichment at C-4 in asp from higher plants measured by Melzer and O'Leary (1987, 1991) was interpreted as indicating partial formation of OAA by PEP carboxylase with the remainder coming from the TCA cycle. Macko *et al.* (1987) did not measure intramolecular patterns in their cyanobacterial products, but the enrichment found by Abelson and Hoering (1961, see Fig. 15) was about 13‰. For the particular case of asp, the latter analyses represent both the C-1 and C-4 carboxyl groups. If the enrichment were localized at C-4, it might have been as great as 26‰ and thus approached the relationship indicated in Fig. 17.

The pathways leading to other members of the aspartic acid family are shown in Figure 18. Isotopic compositions of three of these, thr, ile, and lys, are shown in Figure

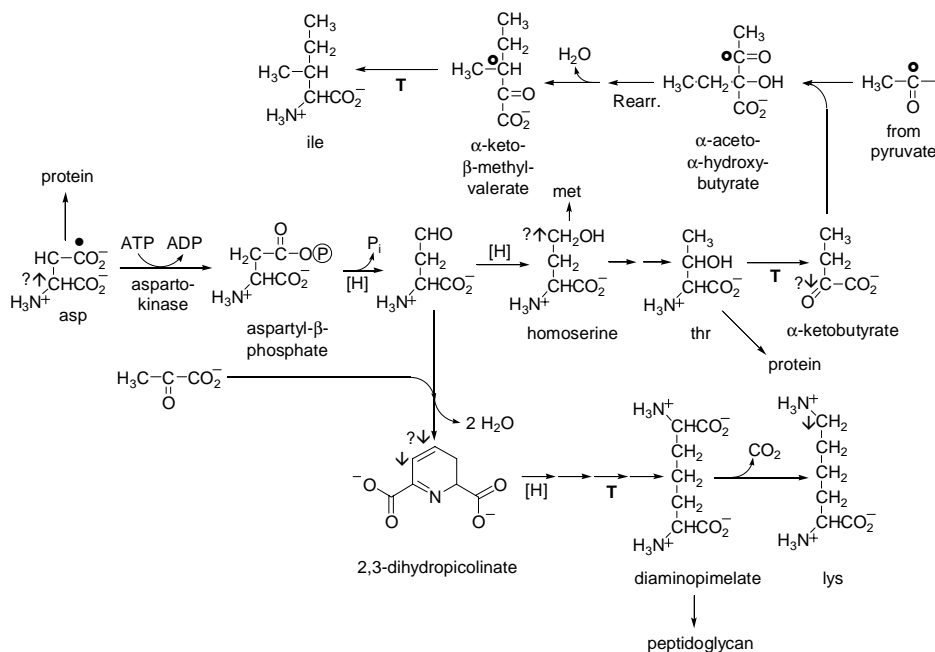


**Figure 18.** Biosynthetic pathways for amino acids in the aspartate family. Circled Ps represent phosphate groups,  $PO_3^{2-}$ .  $P_i$  represents inorganic phosphate,  $HPO_4^{2-}$ . [H] indicates reduction. T indicates transamination. Branch points and likely sites of isotopic fractionation are discussed in the text. In this and other reaction schemes, filled and open circles mark positions enriched or depleted in  $^{13}C$  as a result of the source of the carbon flowing to that position. Upward and downward arrows mark positions likely to be enriched or depleted in  $^{13}C$  relative to precursor positions as a result of fractionations induced by isotope effects.

14. Threonine (thr) retains all of the C present in asp. Why is it not similarly enriched? In fact, thr, ile, and lys are all significantly depleted in  $^{13}C$  relative to asp. The first branch point occurs at asp itself, which can be used either to produce other amino acids or to synthesize proteins. A large isotope effect at C-4 in the production of aspartyl-b-phosphate could wholly or partly neutralize enrichment of  $^{13}C$  at that position. But an isotope effect associated with the attachment of C-1 to aspartyl-transfer RNA via an ester linkage, the first step in protein synthesis, could lead to enrichment of  $^{13}C$  at C-1. The second branch point occurs at  $\beta$ -aspartyl semialdehyde, which can flow either to homoserine or, with addition of pyruvate, to a seven-carbon intermediate that is rapidly cyclized to form 2,3-dihydropicolinate. Fractionation at this point could explain the depletion of  $^{13}C$  in thr relative to asp, but would have the effect of sending a  $^{13}C$ -enriched stream toward lys, which is in fact even more strongly depleted. The 2,3-dihydropicolinate is later opened to yield diaminopimelate. The reactions leading from  $\beta$ -aspartyl semialdehyde to diaminopimelate add carbon that dilutes the enrichment at C-4 in asp and involve very significant changes in bonding at four carbon atoms. These processes and a further branch point at which diaminopimelate can be used to produce peptidoglycan (of which it is an important constituent in Gram-negative bacteria and in cyanobacteria) must play a role in explaining the depletion of  $^{13}C$  in lys. A third branch point occurs at homoserine. Both paths involve largely irreversible reactions at the OH group (phosphorylation, acylation).

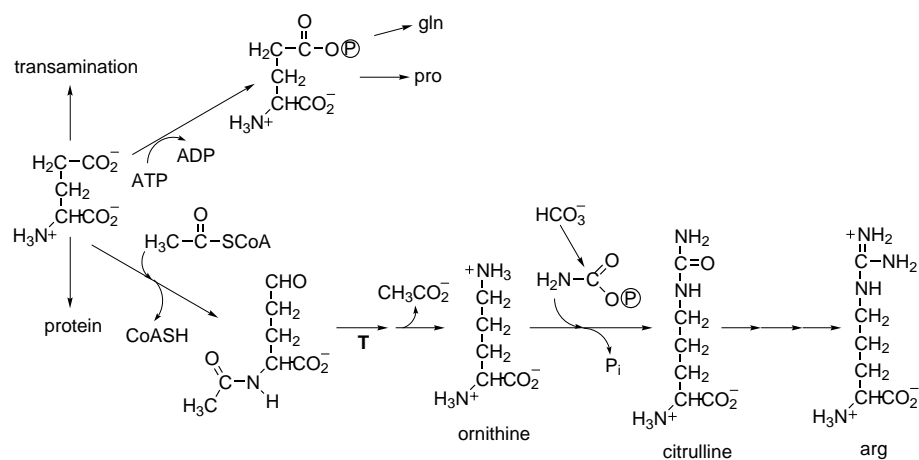


**Figure 19.** Biosynthetic pathways for amino acids in that glutamate family. Abbreviations as in Figure 18. The reactant formed from bicarbonate and used in the production of citrulline is carbamoyl phosphate.

Significant isotopic fractionations are not likely.

Isoleucine (ile) is the last member of the aspartic acid family represented in Figure 14. Two processes are potentially responsible for its depletion in  $^{13}\text{C}$  relative to thr. The first lies at the thr branch point (Fig. 18), where an isotope effect on the transamination leading to  $\alpha$ -ketobutyrate could lead to depletion of  $^{13}\text{C}$  at C-2 in that product. The second is the addition of an acetyl group to produce aceto-a-hydroxybutyrate. The carbonyl position in the acetyl group is likely to be depleted in  $^{13}\text{C}$  (Melzer and Schmidt, 1987).

Two members of the  $\alpha$ -ketoglutarate family of amino acids are represented in Figure 14. Carbon in glu + glx (glx) is only slightly less strongly enriched in  $^{13}\text{C}$  than asp. The intramolecular analyses which, in the case of glx, refer only to C-1, indicate enrichment of nearly 20% at that position. Tracking this carbon backward through the TCA cycle leads to C-4 of OAA. Comparison to the carboxyl-group enrichment measured for the sum of positions C-1 and C-4 in asp (Fig. 15) suggests that most of the excess

$^{13}\text{C}$  in OAA must have been at C-4. As indicated in Figure 19, at least four pathways lead away from newly synthesized glu. Any kinetic isotope effect associated with transamination (in which glu serves as the  $\text{NH}_2$  source for the synthesis of other amino acids) would enrich C-2. Any isotope effect associated with production of glutamate-5-phosphate has the potential to enrich C-5. While both of these mechanisms might contribute to the enrichment observed in glu, the first step leading toward ornithine and ultimately to arginine involves a reaction at the amino group and is not likely to cause

any carbon-isotopic fractionation. Moreover, from that point, no carbon is removed from the set of atoms flowing to arg and only one, for which serves as the source, is added. The depletion of  $^{13}\text{C}$  in arg is thus unexplained.

Valine (val), alanine (ala), and leucine (leu) are members of the pyruvate family. Their biosynthetic pathways are summarized in Figure 20. Pyruvate is closely related to the  $\text{C}_3$  products of photosynthesis. At least one major pathway leading from it, the production of acetyl groups by pyruvate dehydrogenase, has a significant carbon kinetic isotope effect (Melzer and Schmidt, 1987). The slight enrichment observed in ala relative to the estimated isotopic composition of photosynthate fits into this picture nicely. As shown (Fig. 20), val is produced by addition of an acetyl group to the ala carbon skeleton. In spite of the expectation that this acetyl group would be depleted in  $^{13}\text{C}$  relative to the pyruvate, val is slightly enriched in  $^{13}\text{C}$  relative to ala. The branch point at  $\alpha$ -ketoisovalerate provides an opportunity for the required fractionation. A carbon kinetic isotope effect at C-2 in that intermediate would send a  $^{13}\text{C}$ -depleted stream to leu and a relatively enriched stream

to val. The average content of  $^{13}\text{C}$  in leu would be further decreased by the addition of a  $^{13}\text{C}$ -depleted acetyl group. Leucine is the only amino acid which derives its carboxyl group from the carboxyl position in acetate. The uniquely large depletion of  $^{13}\text{C}$  in the carboxyl group of leu from heterotrophic organisms (Fig. 15) provided the first evidence for the large carbon kinetic isotope effect associated with pyruvate dehydrogenase, now held responsible for the depletion of  $^{13}\text{C}$  in *n*-alkyl lipids (DeNiro and

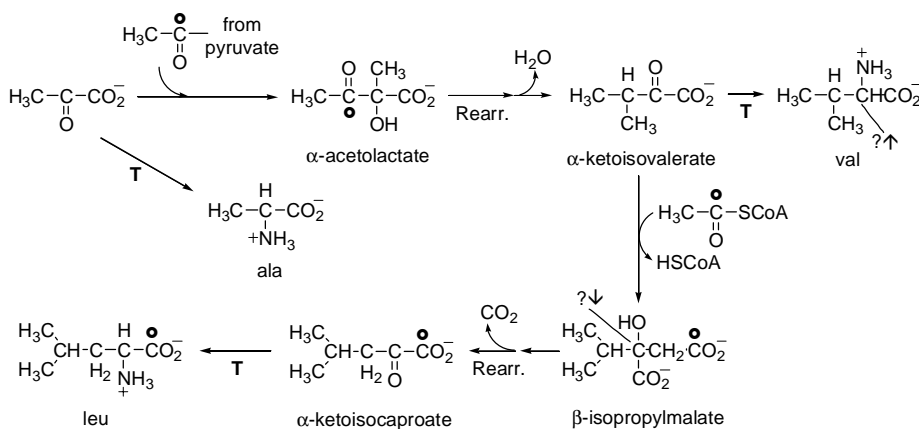


**Figure 20.** Biosynthetic pathways for amino acids in the pyruvate family. Abbreviations as in Figure 18.

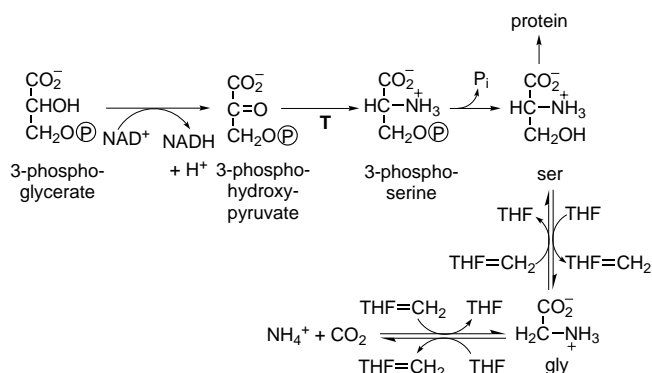


**Figure 21.** Biosynthetic pathways for amino acids in the 3-phosphoglycerate family. THF represents tetrahydrofolate, a cofactor which can accept and donate methylene groups. Other abbreviations as in Figure 18.

Epstein, 1977; Monson and Hayes, 1982a). Notably, the carboxyl group of leu from photoautotrophs is *not* commonly depleted in <sup>13</sup>C (Fig. 14). It follows that the overall depletion of <sup>13</sup>C in leu must be due also to depletions at other sites within the molecule.

Serine (ser) and glycine (gly) are members of the phosphoglycerate family, for which biosynthetic pathways are summarized in Figure 21. A close isotopic relationship to photosynthate would be expected, but ser is enriched by roughly 5‰ (Fig. 14; even larger enrichments have been reported by Abelson and Hoering, 1961, and by Winters, 1971). Particularly because there is no evidence for strong enrichment of <sup>13</sup>C in the carboxyl group (Fig. 15), attention is due to the reaction by which gly is produced from ser. In it, C-3 of serine is transferred to tetrahydrofolate, from which it flows to provide C<sub>1</sub> units in a wide variety of biosynthetic reactions. A significant isotope effect associated with the transfer would be consistent with the enrichment of <sup>13</sup>C in ser relative to gly and with the relationships of these products to photosynthate.

The aromatic amino acids, phe and tyr remain. Their carbon derives from phosphoenolpyruvate and erythrose-

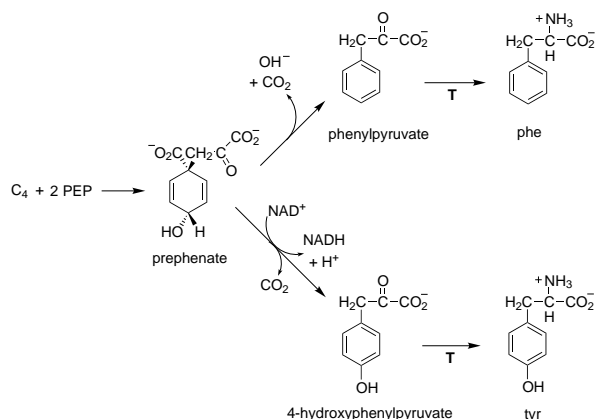


**Figure 22.** Terminal stages of the biosyntheses of the aromatic amino acids phe and tyr. As noted in the text, it is unlikely that isotope effects associated with this branch point alone can account for the isotopic difference observed between phe and tyr.

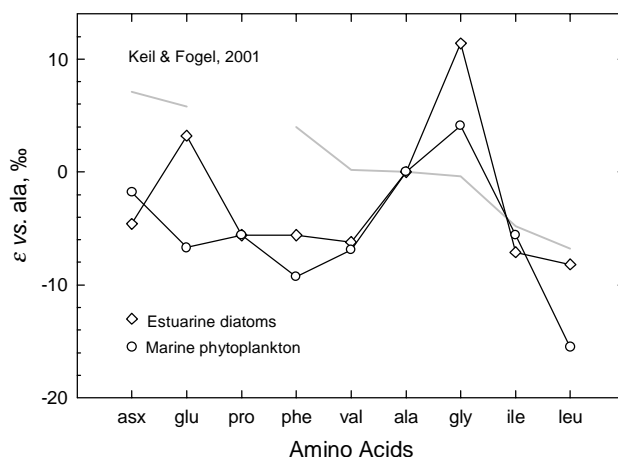


**Figure 23.** Isotopic compositions of amino acids, expressed as fractionations relative to alanine, from natural populations of estuarine diatoms and marine phytoplankton analyzed by Keil and Fogel (2001). For comparison, the heavy gray line depicts the average of the analyses reported in Figure 14. The  $\epsilon$  range is identical to that in Figure 14. The horizontal scale covers only the amino acids analyzed by Keil and Fogel (2001).

4-phosphate. As required by the large, structural differences between those materials and the aromatic amino acids, there are many reactions between the biosynthetic feedstocks and the ultimate products. All but one of these, however, affect both phe and tyr which, as shown in Figure 22, share an immediate precursor. It is not possible to explain the intermolecular difference of more than 10‰ based on fractionations localized at the OH-bearing carbon in prephenate. The products each contain nine carbon atoms so that the required isotopic difference at that position would be 90‰. Pools of prephenate separated in time or space are indicated.

#### Amino acids *not* from cultured cyanobacteria

Strikingly different isotopic distributions are found when amino acids from multicellular plants or from natural populations of algal unicells are analyzed. In general, the trend to greater downstream depletion discernible in Figure 14 is less marked. The generally flatter isotopic distribution is, however, interrupted by some notable enrichments and depletions. These points, along with some notable inconsistency and variability, are exemplified by the distributions shown in Figures 23 and 24. Amino acids in the sequence from asx to ala are commonly depleted and those in the sequence from ala to lys are commonly enriched relative to the trend defined by *Anabaena*. One feature of this flattening is removal of the puzzling isotopic contrast between phe and tyr. Notable enrichments of <sup>13</sup>C appear frequently in gly. On the other hand, the depletion of <sup>13</sup>C in leu noted originally in the *Anabaena* data appears to be a robust feature.

The turnover of amino acids in microbial cultures increases in stationary phase. If it is, at least, more important during slow growth and under natural stresses, it fol-

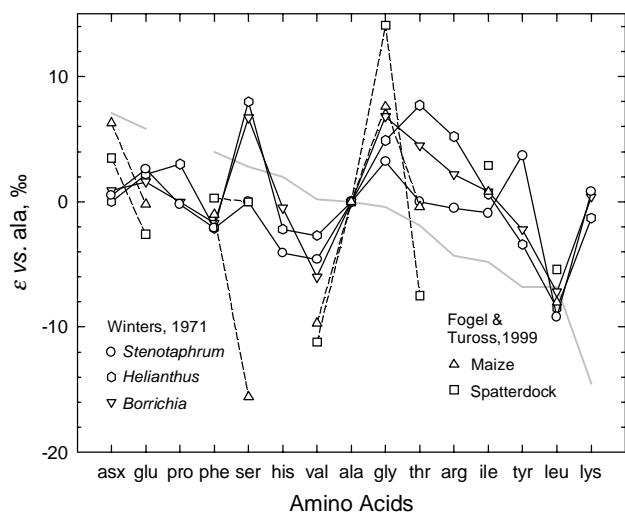


**Figure 24.** Isotopic compositions of amino acids, expressed as fractionations relative to alanine, from the vascular plants *Stenotaphrum* (St. Augustine grass), *Helianthus* (sunflower), and *Borrichia* (sea daisy) reported by Winters (1971) and from maize and spatterdock reported by Fogel and Tuross (1999). For comparison, the heavy gray line depicts the average of the analyses reported in Figure 14.

lows that isotopically depleted products from the ends of the biosynthetic pathways will be recirculated more frequently than in the continuously illuminated, optimal cultures of *Anabaena*. Greater recycling will reduce the removal of carbon skeletons from the tricarboxylic acid cycle and result in the importation of less  $^{13}\text{C}$ -enriched material from that source. Together, these processes should lead to the accumulation of  $^{13}\text{C}$ -enriched residues at the ends of the biosynthetic pathways and to the delivery of  $^{13}\text{C}$ -depleted feedstocks to the first steps in the pathways.

The enrichment of  $^{13}\text{C}$  in gly is probably linked to  $\text{C}_1$  metabolism. As shown in Figure 21, methylene groups for use in other biosynthetic processes can be produced by the  $\text{ser} \rightarrow \text{gly}$  and  $\text{gly} \rightarrow \text{CO}_2 + \text{NH}_4^+$  pathways. Conversely, if  $\text{THF}=\text{CH}_2$  is in oversupply, it can be consumed *via* reversal of those pathways. As a result, isotopic relationships between gly, ser, and the other amino acids should respond to production or consumption of  $\text{THF}=\text{CH}_2$ . Enrichment of  $^{13}\text{C}$  in gly relative to ser seems most likely to reflect synthesis of gly from  $\text{CO}_2$ ,  $\text{NH}_4^+$ , and  $\text{THF}=\text{CH}_2$ .

### Isotopic Compositions of Nucleic Acids

The nucleic acids are polynucleotides. Each nucleotide contains one phosphate group, a  $\text{C}_5$  sugar (ribose or deoxyribose), and an aromatic, heterocyclic "base," either a one-ring pyrimidine (four or five carbon atoms + N, O, and H) or a two-ring purine (five carbon atoms + N, O, and H). The carbon isotopic compositions of nucleic acids, therefore, are expected to represent an average of the ribose and the bases. In the four-carbon pyrimidines uracil and cytosine, three carbons come from C-2, 3, and 4 from asp and the fourth comes from carbamoyl phosphate (see

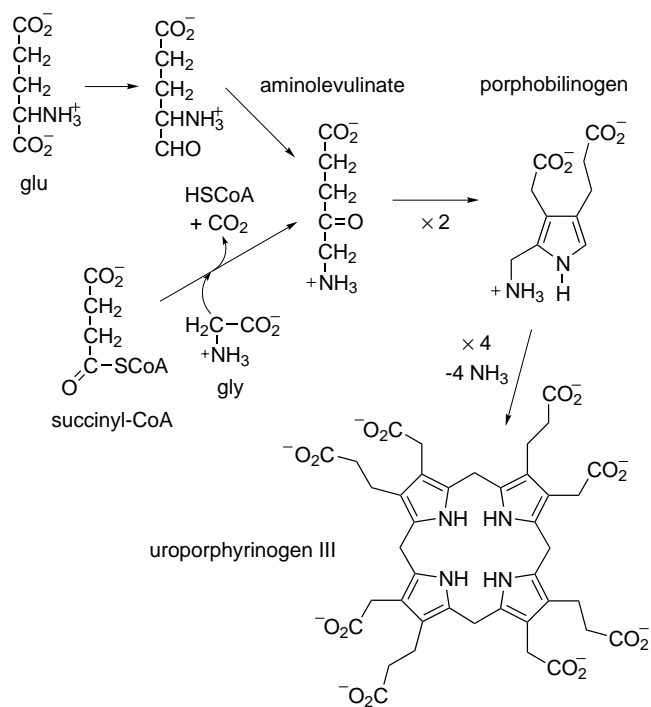


**Figure 25.** Diagram summarizing the relationships between carbon atoms in a tetrapyrrole ring system and in various precursors, either glu or succinate + the methylene carbon in gly.

structure in Fig. 19). The five-carbon pyrimidine thymidine adds one C from a tetrahydrofolate carrier (*cf.* discussion of the biosynthesis of glycine). The inclusion of C-4 from asp and the insertion of C from carbamoyl phosphate, for which serves as the carbon source, both suggest that the pyrimidines, with the possible exception of thymidine, would be enriched in  $^{13}\text{C}$  relative to photosynthate. The purines contain both carbons from gly, two  $\text{C}_1$  units from THF, and a C from  $\text{CO}_2$ . If one dared to make a prediction about such a salad, it would be that it was depleted in  $^{13}\text{C}$  relative to photosynthate.

Observations indicate that the enrichments in the pyrimidines (likely, but of unknown magnitude) and the depletions in the purines (hypothetical, but apparently needed to explain the results) balance at least roughly. Pioneering analyses of the carbon-isotopic compositions of bacterial nucleic acids were reported by Blair *et al.* (1985), who found nucleic acids enriched in  $^{13}\text{C}$  relative to biomass by 0.6‰. More recently, this work has been very nicely extended by Richard Coffin and his coworkers, who report that bacterial nucleic acids are enriched relative to biomass by about 0.3‰ (Coffin *et al.*, 1990). The isotopic compositions closely follow those of heterotrophic carbon sources, and this can be exploited to provide new information about the roles of bacteria in aquatic food webs (Coffin *et al.*, 1994; 1997).

### Isotopic Compositions of Tetrapyrroles

The heteroaromatic ring system in chlorophyll is a prominent tetrapyrrole and is of particular interest since related

products are often preserved in sediments as porphyrins. As shown in Figure 25, its immediate precursor is aminolevulinic acid ( $C_3$ ) which is in turn synthesized from glycine and succinyl-CoA with loss of  $CO_2$  ( $C_2 + C_4 \rightarrow C_5 + C_1$ ) or from glutamate ( $C_3$ ). The carbon flowing to tetrapyrroles is thus closely related to that in amino acids and in intermediates from the TCA cycle and is expected to have an isotopic composition close to that of biomass. In specific analyses of chlorophyllides (*i. e.*, the non-phytol carbon from chlorophyll) from the photosynthetic bacteria *Rhodospseudomonas capsulata* and *Chromatium vinosum*, Takigiku (1987) found enrichments of 0.0 and 0.7‰ relative to biomass. Chloroplasts from beech tree leaves used to test procedures in the same investigation also yielded chlorophyllides enriched in  $^{13}C$  relative to plastid biomass by 0.7‰. Madigan *et al.* (1989) found chlorophyllides from *Chromatium tepidum* enriched in  $^{13}C$  by 0.5‰ relative to biomass. Considering diverse analyses that provided indirect evidence about the isotopic compositions of chlorophyllides relative to biomass, Laws *et al.* (1995) and Bidigare *et al.* (1999) concluded that 0.5‰ was a good estimate of the enrichment of chlorophyllides relative to biomass in marine plankton. In a single investigation of chlorophyllide from a cyanobacterium, *Synechocystis* sp., Sakata *et al.* (1997) found an enrichment of 2.7‰ relative to biomass and attributed the difference to shifted carbon flows that increased the abundance of proteins relative to lipids and other cellular components in cyanobacteria.

### Isotopic Compositions of Lipids

Lipids have either linear or isoprenoidal carbon skeletons. All of the linear skeletons derive from the same biosynthetic pathway but there are two ways to produce isoprenoids, one of which has been discovered so recently that it is not mentioned in standard textbooks. The linear, or *n*-alkyl, lipids are often termed “acetogenic” because of their relationship to acetate, which is both their immediate biosynthetic precursor and the main product of their metabolic degradation. Structural variations within the acetogenic lipids are exemplified in Figure 26. Products containing no hydrolyzable linkages are “simple lipids,” those

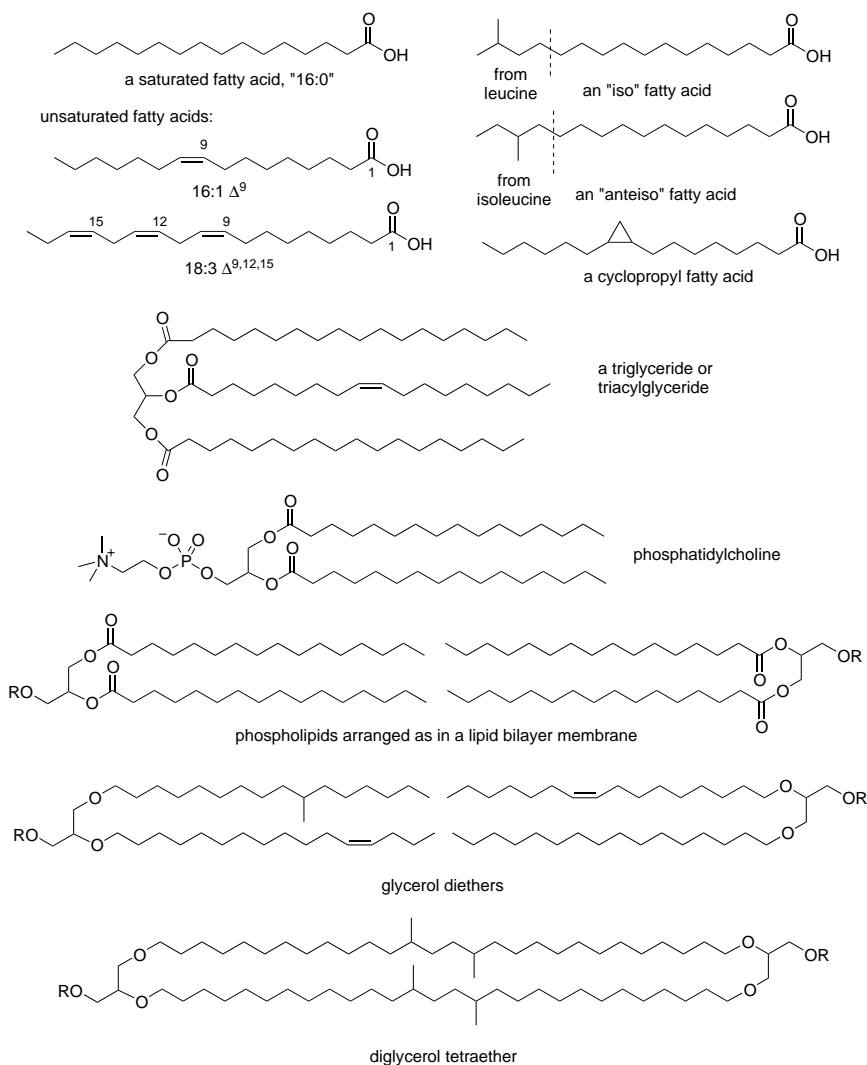


**Figure 26.** Representative *n*-alkyl, or “acetogenic” lipids. Each linear carbon skeleton is built up from  $C_2$  units supplied in the form of acetyl-CoA. The saturated carbon skeletons represented here by carboxylic acids also occur commonly as alcohols. As shown, lipid bilayer membranes are comprised of diglycerides with polar “head groups” represented by R in the shorthand structures shown in the lower portion of the figure. An example of a polar head group is shown in the structure of phosphatidylcholine. Although ester linkages are most common in complex lipids, ether linkages are being recognized with increasing frequency among bacterial products (Hayes, 2000).

containing one or more ether or ester bonds are “complex lipids.” As shown, structural variations that affect the carbon skeleton are restricted to methyl branching and rare, cycloalkyl substituents.

The structural range of isoprenoid carbon skeletons is far greater. All are based on the isoprene, but there are two means of variation: (1) the connections between isoprene units, whether head-to-tail, head-to-head, tail-to-tail, or irregular (involving isoprene positions C-2 or C-3); and (2) cyclization. Only the first of these is considered in Figure 27. Assuming that no carbon atoms have been added to or trimmed from the basic carbon skeleton, the carbon number for any isoprenoid is some multiple of five. A  $C_{10}$  isoprenoid is a monoterpene, a  $C_{15}$  is a sesquiterpene, a  $C_{20}$

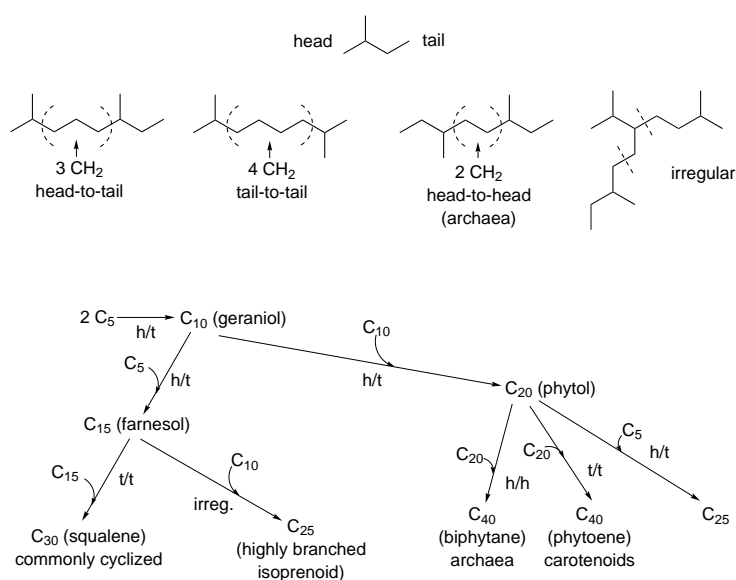


**Figure 27.** Molecular structures showing the that junctions between isoprene units can be recognized by counting the number of  $\text{CH}_2$  groups between methyl branches. The branching diagram indicates biosynthetic relationships between various isoprenoid carbon skeletons. Names of typical products appear in parentheses (*n. b.*, geraniol and phytol are merely examples and are far from the only  $\text{C}_{10}$  and  $\text{C}_{20}$  isoprenoids). The irregular-junction case is an example based on Rowland *et al.* (1995)

is a diterpene... *etc.* In eukaryotic plants, including phytoplankton, the  $\text{C}_{20}$  and  $\text{C}_{40}$  isoprenoids are formed in the chloroplast and the  $\text{C}_{30}$  products are of cytosolic origin. The head-to-head linkage is generally restricted to the Archaea.

Turning to cyclization, isolated rings are common in  $\text{C}_{40}$  isoprenoid structures (carotenoids and archaeal tetraethers) but are not key points of classification. Structures with more than two fused rings are almost exclusively restricted to isoprenoids based on squalene (gibberelins, based on phytol, are a rare exception). Two major classes – tetracyclic and pentacyclic – are shown in Figure 28. Sterols are tetracyclic structures that are important constituents of all eukaryotic membranes. Although they have been widely reported as present in heterotrophic bacteria and cyanobacteria (see, for example, references cited by Kohl *et al.*, 1983), proven instances of their *biosynthesis* are limited to aerobic, methanotrophic bacteria (Bird *et al.*, 1971; Summons *et al.*, 1994) and to *Nannocystis exedens* (Kohl *et al.*, 1983). The emphasis on biosynthesis, demonstrated by transmission of an isotopic label from a precursor to steroidal products stems from (1) the demonstration by Levin and Bloch (1964) that sterols isolated from cyanobacterial cultures were not biosynthetic products but instead contaminants apparently derived from the media and (2) the observation that some bacteria which incorporate sterols in their membranes nevertheless require an exogenous source for the sterolic carbon skeleton (Razin, 1978). Pentacyclic isoprenoid alcohols, often with highly polar, non-lipid substituents that raise their carbon number to 35 or more, are produced by many aerobic bacteria and

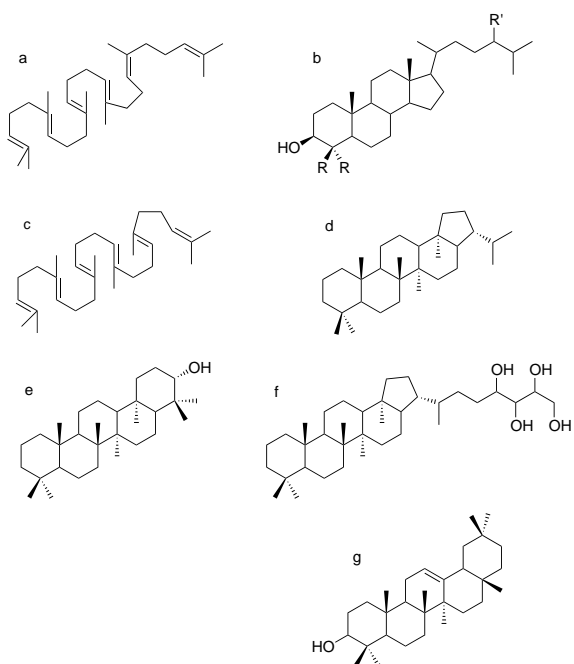


**Figure 28.** Cyclic isoprenoid lipids and their relationships to squalene. (a) Squalene folded so as to demonstrate its relationship to a sterol carbon skeleton (b). In sterols that occur commonly, some of the methyl groups resulting from the cyclization of squalene move from one carbon to another and others are lost. The substituents marked R can be either methyl or H and the substituent marked R' can be H, methyl, ethyl, or propyl. In specific natural products, double bonds often occur within the ring system. (c) Squalene folded so as to demonstrate its relationship to the pentacyclic ring systems in structures d, e, and f. (d) The hopane carbon skeleton. (e) Tetrahymanol. (f) Bacteriohopane tetrol, an extended hopanoid that includes five carbons deriving from the  $\text{C}_5$  sugar ribose. (g)  $\beta$ -Amyrin, a typical pentacyclic isoprenoid produced by higher plants.

apparently serve as sterol surrogates in their membranes (Rohmer *et al.*, 1984). The dominant family of products is based on the hopane carbon skeleton (Fig. 28). Two additional groups of pentacyclic triterpenoids are comprised entirely of six-membered rings. Those with an OH group on the fifth ring are commonly products of protozoans. Tetrahymanol (Fig. 28) is a prominent example (Raederstorff and Rohmer, 1988). A thus-far-unique bacterial occurrence of this compound has also been reported in *Rhodopseudomonas palustris* (Kleeman *et al.*, 1990). Pentacyclic triterpenoids with an OH group on the first ring are commonly products of higher plants.

### Processes affecting the carbon-isotopic compositions of *n*-alkyl lipids

*n*-Alkyl carbon skeletons are essentially acetate polymers derived from acetyl-coenzyme A. In plants and in heterotrophs, that building block is formed by the oxidative decarboxylation of pyruvate, which is produced by the degradation of carbohydrates (including the immediate,  $\text{C}_3$

products of photosynthesis). The reaction is catalyzed by pyruvate dehydrogenase and is associated with a significant, carbon kinetic isotope effect (Melzer and Schmidt, 1987). Because pyruvate has multiple fates, isotopic fractionation is expected and, in fact, the general depletion of  $^{13}\text{C}$  in *n*-alkyl lipids has been attributed to this step (DeNiro and Epstein, 1977; Monson and Hayes, 1982a). Additional factors must be important and may help to explain variations in lipid isotopic compositions (Blair *et al.*, 1985). These factors include variations in the branching ratios at pyruvate; alternate sources of acetyl-CoA, which is also produced by the degradation of some amino acids (ile, leu, thr, and trp); and downstream isotope effects. Acetyl-CoA itself has multiple fates. If the reaction pathways competing for it have different isotope effects, the isotopic compositions of the *n*-alkyl lipids will vary from that of the acetyl-CoA. The fates include oxidation to  $\text{CO}_2$  via the TCA cycle; biosynthesis of some amino acids (leu, lys); the production of *n*-alkyl-lipid carbon skeletons; the production of mevalonic acid, a precursor of isoprene; and, in many aquatic unicells, hydrolysis to yield acetate which leaks from the cell before being utilized (Roberts *et al.*, 1955; Blair *et al.*, 1985).

The site of fatty-acid synthesis varies very significantly. If a cell has chloroplasts – if it is an algal unicell or a carbon-fixing cell within a differentiated photoautotroph – all fatty acids with 18 or fewer carbon atoms are produced within it (Cavalier-Smith, 2000). If a cell lacks chloroplasts the fatty acids are produced in the cytosol using (in eukaryotic cells) acetate exported from the mitochondria. The consequences of these points can be discussed more completely and systematically in parallel with a consideration of isoprenoid lipids.

### Processes affecting the carbon-isotopic compositions of isoprenoid lipids

The isoprene carbon skeleton is indicated schematically in Figure 27. The corresponding biosynthetic reactant – equivalent in its role to acetyl-CoA – is isopentenyl pyrophosphate. As shown in Figure 29, this compound can be made by two different and fully independent pathways. The mevalonic-acid pathway was until recently thought to be the only route to isoprenoids. The deoxyxylulose-phosphate, or methylerythritol-phosphate, pathway was first discovered in Bacteria by Rohmer and coworkers (Flesch and Rohmer, 1988; Rohmer *et al.*, 1993). Subsequent investigations (reviewed by Lichtenthaler, 1999) have shown that this pathway is widely distributed in prokaryotes, in the chloroplasts of eukaryotic algae and higher plants, and in the cytosol of members of the Chlorophyta (including the Trebouxiophyceae, Chlorophyceae, and Ulvophyceae; see summary in Table 4 and note very recent clarification by Schwender *et al.*, 2001). In contrast to acetyl-CoA, isopentenyl pyrophosphate is a dedicated product flowing only to the biosynthesis of a single class of lipids. The isotopic compositions of the polyisoprenoid lipids will therefore be controlled by the isotopic composition of the isopentenyl pyrophosphate.

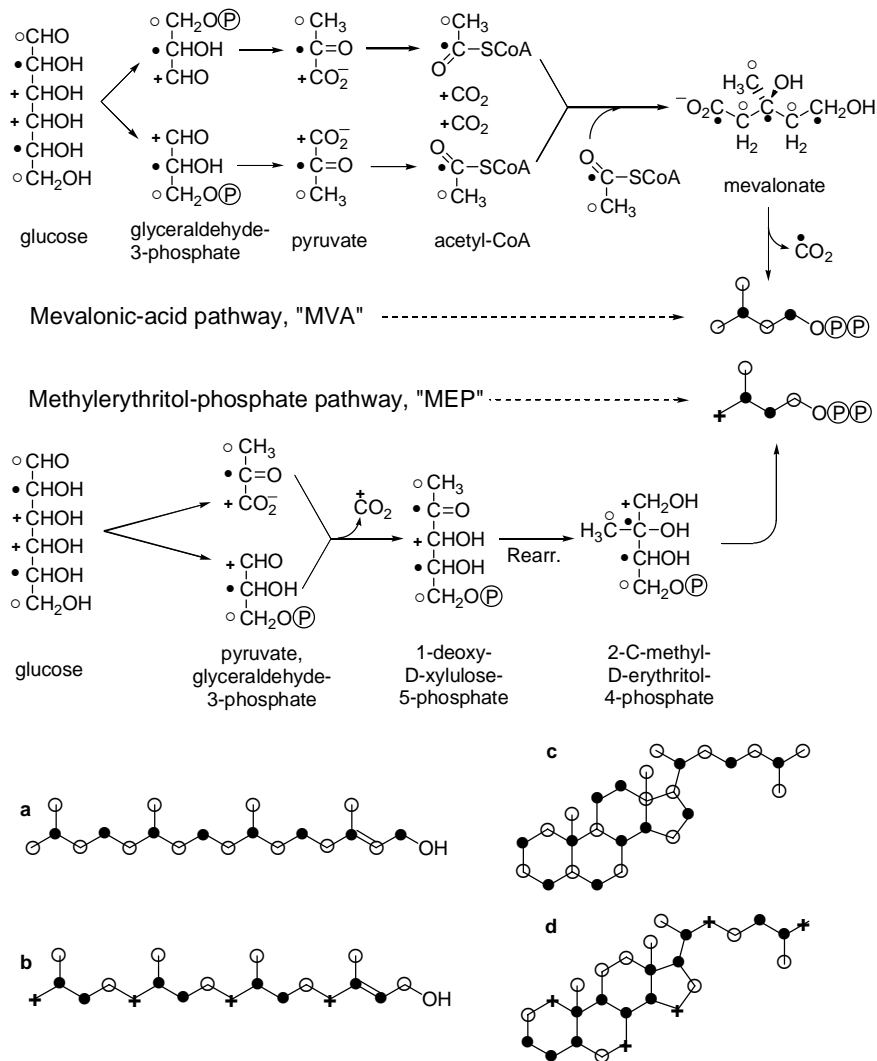


**Figure 29.** Relationships between the carbon positions in isopentenyl pyrophosphate and their sources. In the mevalonic-acid pathway, all five carbon positions in isopentenyl pyrophosphate derive from acetate and, in turn, from the C-1 + C-6 and C-2 + C5 positions of glucose. In the methylerythritol-phosphate pathway, one carbon derives from the C-3 + C-4 position in glucose. The mapping of positions from precursors into products of the two pathways differs sharply, as indicated by structures of acyclic and steroidal carbon skeletons based on the MVA (a, c) and MEP pathways (b, d).

phate, or methylerythritol-phosphate, pathway was first discovered in Bacteria by Rohmer and coworkers (Flesch and Rohmer, 1988; Rohmer *et al.*, 1993). Subsequent investigations (reviewed by Lichtenthaler, 1999) have shown that this pathway is widely distributed in prokaryotes, in the chloroplasts of eukaryotic algae and higher plants, and in the cytosol of members of the Chlorophyta (including the Trebouxiophyceae, Chlorophyceae, and Ulvophyceae; see summary in Table 4 and note very recent clarification by Schwender *et al.*, 2001). In contrast to acetyl-CoA, isopentenyl pyrophosphate is a dedicated product flowing only to the biosynthesis of a single class of lipids. The isotopic compositions of the polyisoprenoid lipids will therefore be controlled by the isotopic composition of the isopentenyl pyrophosphate.

Isotope effects potentially associated with the syntheses of mevalonic acid or of methyl-erythritol have not been directly investigated. Nor have intramolecular patterns of isotopic order been measured in polyisoprenoids. As a result, stepwise or process-related isotopic fractionations associated with the biosynthesis of polyisoprenoid lipids can only be estimated from observed isotopic compositions of whole molecules.

### Carbon isotopic compositions of lipids from heterotrophic bacteria

Four separate investigations of carbon isotopic fractionation in aerobic growth of *Escherichia coli* provide consistent and complementary results that provide a foundation for understanding the isotopic compositions of lipids. DeNiro and Epstein (1977) grew separate cultures of *E. coli* using glucose, pyruvate, and acetate as carbon sources. "Lipids" produced by the bacteria were depleted in  $^{13}\text{C}$  by 6-8‰ relative to glucose or pyruvate but nearly unfractionated relative to acetate. Accordingly, they concluded that the reaction that produced acetate from pyruvate must be responsible for the depletion of  $^{13}\text{C}$  in lipids. To examine that process specifically, they made site-specific analyses of all of the carbon positions in the reactants and products, substituting readily available yeast pyruvate carboxylase for *E. coli* pyruvate dehydrogenase. They found normal kinetic isotope effects at all carbon positions in pyruvate:  $\epsilon_{\text{C-1}} = 7.8$ ,  $\epsilon_{\text{C-2}} = 14.7$ , and  $\epsilon_{\text{C-3}} = 1.0$ ‰. C-2 in pyruvate becomes the carboxyl carbon in acetyl-CoA. C-3 becomes the methyl carbon. Because of the strongly differing isotope effects, depletion of  $^{13}\text{C}$  at the carboxyl position should be 15 times greater than that at the methyl position. The chain of chemically indistinguishable  $\text{CH}_2$  groups within the fatty acid should contain two isotopically distinct subsets of carbon atoms, with those derived from the carboxyl carbon being depleted in  $^{13}\text{C}$  relative to those derived from the methyl carbon. The depletion of  $^{13}\text{C}$  in the molecule overall would be the average of the small depletion at the even-numbered positions and the large depletion at the odd-numbered positions.

Monson and Hayes (1980, 1982a) grew *E. coli* on glucose, isolated the individual fatty acids, and used chemical techniques to obtain  $\text{CO}_2$  from specific positions within the molecules. Key reactions produced  $\text{CO}_2$  quantitatively from carboxyl groups (Vogler and Hayes, 1978; 1979) and oxidized double bonds quantitatively to produce carboxyl groups at the terminal positions of cleavage products (Monson and Hayes, 1982a). The double bonds in unsaturated fatty acids produced by *E. coli* do not result from the action of a desaturase enzyme. Instead, even when  $\text{O}_2$  is available,

Table 4. Pathways used for the biosynthesis of isoprenoid lipids

Organism	Pathway	Reference <sup>a</sup>
Prokaryotes		Lange <i>et al.</i> , 2000
Bacteria		Boucher and Doolittle, 2000
Aquificales, Thermotogales	MEP	
Photosynthetic bacteria		
<i>Chloroflexus</i>	MVA	Rieder <i>et al.</i> , 1998
<i>Chlorobium</i>	MEP	Boucher and Doolittle, 2000
Gram positive eubacteria		
Commonly	MEP	
<i>Streptococcus</i> , <i>Staphylococcus</i>	MVA	Boucher and Doolittle, 2000
<i>Streptomyces</i>	MEP & MVA	Seto <i>et al.</i> , 1996
Spirochaetes		Boucher and Doolittle, 2000
<i>Borrelia burgdorferi</i>	MVA	
<i>Treponema pallidum</i>	MEP	
Proteobacteria		
Commonly	MEP	
<i>Myxococcus</i> , <i>Nannocystis</i>	MVA	Kohl <i>et al.</i> , 1983
Cyanobacteria	MEP	Disch <i>et al.</i> , 1998
Archaea	MVA	Lange <i>et al.</i> , 2000
Eukaryotes		
Non-plastid-bearing	MVA	Lange <i>et al.</i> , 2000
Plastid-bearing		
Chlorophyta <sup>b</sup>	Plastid MEP	Schwender <i>et al.</i> , 2001
Streptophyta <sup>c</sup>	Cytosol MEP	Lichtenthaler <i>et al.</i> , 1997
Euglenoids	MVA MVA	Lichtenthaler, 1999

<sup>a</sup> Where no reference is cited, either the assignment is based on generalizations introduced and supported in three major reviews – Lange *et al.* (2000), Boucher and Doolittle (2000), and Lichtenthaler (1999) – or it is based on work cited in those reviews, the first two of which are based on genetic analyses rather than labeling studies.

<sup>b</sup> Chlorophytes include the Trebouxiophyceae, Chlorophyceae, and Ulvophyceae.

<sup>c</sup> Streptophytes include higher plants and eukaryotic algae other than those named above.

they are produced by an anaerobic mechanism that prevents complete hydrogenation of the alkyl chain as it is lengthened during biosynthesis. No mechanism exists for the isotopic fractionation of the doubly bonded carbons – for example, at C-9 and C-10 in *n*-hexadec-9-enoic acid – relative to the other odd- and even-numbered carbon positions in the molecule. Like DeNiro and Epstein (1977), Monson and Hayes (1982a) found that the crude lipids were depleted in  $^{13}\text{C}$  by 7‰ relative to the carbon supplied by glucose. The individual fatty acids were, however, depleted by only 3‰ (the difference being explained by the presence of more strongly depleted neutral components in the lipid fraction). Production of  $\text{CO}_2$  from positions within the carbon chain showed that the odd-numbered carbon positions, derived from the carboxyl group of acetyl-CoA, were depleted relative to the supplied glucose by  $6 \pm 1$ ‰ and that the even-numbered carbon positions, derived from the methyl position of acetyl-CoA, were enriched by  $0.5 \pm 1.4$ ‰. These results decisively confirmed the existence of intramolecular isotopic order in *n*-alkyl lipids. The pattern, moreover, was consistent with the outline provided by De-

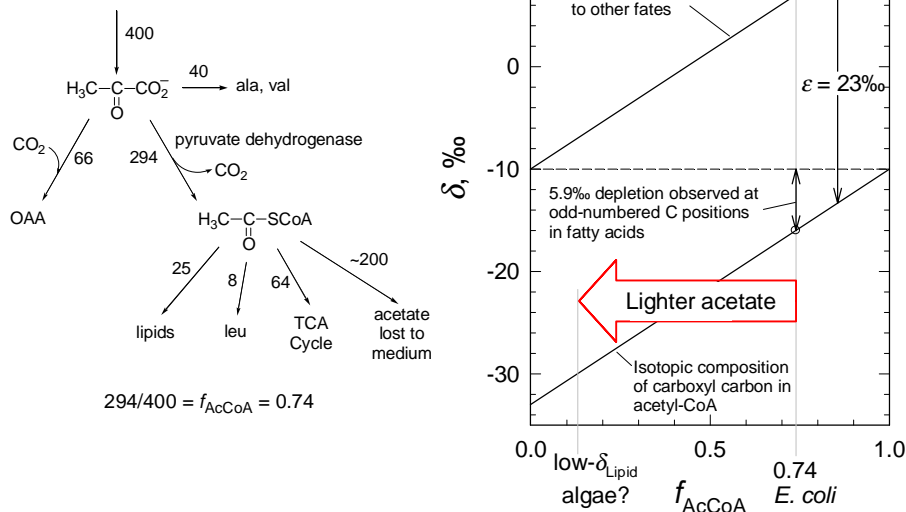


**Figure 30.** Flows of carbon at the pyruvate branch point in the metabolism of *E. coli* growing aerobically on glucose (Roberts *et al.*, 1955). As noted, 74% of the pyruvate is decarboxylated to yield acetyl-CoA. The observed depletion of  $^{13}\text{C}$  at odd-numbered carbon positions in fatty acids (Monson and Hayes, 1982), shown in the graph at the right, therefore indicates that the isotope effect at C-2 in the pyruvate dehydrogenase reaction is 23‰.

Niro and Epstein (1977) in that fractionation was localized at the carboxyl carbon of acetyl-CoA.

To interpret their results quantitatively in terms of isotope effects and reaction pathways, Monson and Hayes (1982a) adopted DeNiro and Epstein's (1977) most basic finding and considered the branch point shown in Figure 30. The existence of well-supported estimates of the carbon flows (Roberts *et al.*, 1955) allowed construction of a fractionation plot based on the assumption that the isotopic composition of C-2 in the pyruvate was equal to that of the glucose supplied to the culture. The resulting fractionation factor, 23‰, is an estimate of the *difference between* the isotope effect at C-2 for pyruvate dehydrogenase *in vivo* and the weighted-average isotope effect at C-2 on the pathways leading to ala, val, and OAA. If those were greater than zero, then  $\epsilon_{\text{C-2}}$  for pyruvate dehydrogenase must be greater than 23‰. The interpretation also assumed that no isotopic fractionation occurred on the pathway leading from acetyl-CoA to fatty acids and that the steady-state isotopic composition of acetyl-CoA was unaffected by any isotope effects associated with the pathways leading from that reactant to leucine, to the TCA cycle, or to acetate leaking from the cell (a point supported in part by the observation that even-numbered carbon positions in the fatty acids were unfractionated). The 23‰ effect was significantly larger than the 15‰ effect found by DeNiro and Epstein (1977), but it pertained to a different enzyme – pyruvate dehydrogenase in *E. coli* rather than pyruvate

decarboxylase from yeast – and to *in-vivo* rather than *in-vitro* conditions.

A third approach was taken by Blair *et al.* (1985) who grew *E. coli* on glucose while obtaining a complete mass balance. They confirmed the finding of Monson and Hayes (1982a) that the fatty acids are depleted in  $^{13}\text{C}$  by 3‰ relative to the glucose carbon supply. In their experiments, however, the excreted acetate was found to be enriched in  $^{13}\text{C}$  relative to the carbon source by 12‰. Intramolecular analyses showed that virtually all of the enrichment was at the carboxyl carbon, which was enriched by 24‰. They also isolated and analyzed citrate (after quickly killing the cells at mid-log phase) and found that it was unfractionated relative to the carbon source. The latter result can be accommodated by proposing that the depletion of  $^{13}\text{C}$  in the acetyl-CoA called for by

the earlier results was neutralized because the citric acid contained not only the depleted acetate but also carbon from  $^{13}\text{C}$ -enriched OAA, the enrichment resulting from utilization of the pyruvate represented by the upper line in the graph shown in Figure 30. The strikingly enriched extracellular acetate, however, remains unexplained. The authors point out that acetate would not only be leaking from the cells but also being reabsorbed by them and that the loss rate indicated in Figure 30 would be the net of those opposing flows. An isotope effect associated with the assimilation of acetate may, therefore, play a role.

In the final investigation, Melzer and Schmidt (1987) simply made a good measurement of the isotope effects associated with pyruvate dehydrogenase from *E. coli*. For  $\epsilon_{\text{C-2}}$  they reported 21‰, in excellent agreement with the estimate provided by Monson and Hayes (1982a). In sum, these four investigations provide a roughly quantitative view of the processes responsible for the depletion of  $^{13}\text{C}$  in *n*-alkyl lipids but also show how many factors might have importances that are not yet understood.

Isotopic fractionations in lipid biosynthesis during aerobic and anaerobic growth of *Shewanella putrefaciens* on lactate have recently been compared by Teece *et al.* (1999). Under aerobic conditions, fatty acids were depleted in  $^{13}\text{C}$  relative to biomass by 2-3‰, roughly duplicating the characteristics of *E. coli* discussed above. In contrast, fatty acids produced under anaerobic conditions were depleted in  $^{13}\text{C}$  by 5-10‰ relative to biomass. Earlier, Scott

and Nealson (1994) had concluded that, under anaerobic conditions, *S. putrefaciens* metabolized lactate to yield acetyl-CoA and formate, with most of the acetate being excreted and a portion of the formate being assimilated via the serine pathway. If the latter pathway were fully functional, it would provide a second source of acetyl-CoA. The carboxyl carbon in that product is derived from via PEP carboxylase, but Teece *et al.* (1999) do not report the isotopic composition of the CO<sub>2</sub> in their cultures. Together, the metabolic and isotopic investigations provide an excellent demonstration of anaerobic-bacterial complexity and its related hazards. Good work has led to good data but not to firm conclusions. The wide range of depletions (5-10‰) might indicate varying contributions from the two sources of acetyl-CoA (*i. e.*, lactate and the serine pathway). The relatively large depletion must be kept in mind when considering the isotopic compositions of fatty acids in natural systems.

### Carbon isotopic compositions of lipids from cyanobacteria

Although prokaryotic and thus uncompartimentalized, cyanobacteria differ from the organisms just considered in that they are photosynthetic, and thus obtain from light much of the energy required to drive biosynthesis. Moreover, they produce isoprenoidal as well as *n*-alkyl lipids. Sakata *et al.* (1997) recently reported results of the first investigation of lipid-biosynthetic fractionations in a cultured cyanobacterium, specifically *Synechocystis*, which uses the MEP pathway for synthesis of isoprenoids (Lichtenthaler *et al.*, 1997; Disch *et al.*, 1998).

Extractable *n*-alkyl lipids were depleted in <sup>13</sup>C relative to total biomass by 9.1‰, a fractionation three times greater than that in *E. coli*. If localized at the odd-carbon positions, the depletion of 18‰ would require  $f_{\text{AcCoA}} = 0.22$  (see Fig. 30). Factors suggested as responsible for the 3.4-fold decrease in  $f_{\text{AcCoA}}$  were (i) much lower needs for acetyl-CoA in energy production via the TCA cycle and (ii) very low concentrations of lipids in *Synechocystis* (2% of biomass C). These are good points, but it will not be surprising if further investigations show that the large depletion is due to multiple factors.

Three subsets of polyisoprenoids, shown in Figure 31, were analyzed. Phytol, which accounted for 90% of the total polyisoprenoids and 1% of biomass C, was depleted relative to biomass by 6.8‰. Diplopterol and diploptene, comprising 0.04% of biomass C, were similarly depleted (6.9, 6.5‰). Bishomohopanol (0.2% of biomass C), a degradation product of bacteriohopanepolyol, was depleted by 8.5‰. The latter result is striking because, as noted in Figure 31, bishomohopanol contains two carbons that are derived from carbohydrate (Rohmer, 1993) and which are expected to be enriched in <sup>13</sup>C relative to lipid carbon. It suggests that the triterpenoid portion of the bishomohopanol is significantly more strongly depleted ( $\approx 9\%$ ) than the other isoprenoids. Noting that phytol, diplopterol, and diploptene were all resident mainly in membranes and that the abun-

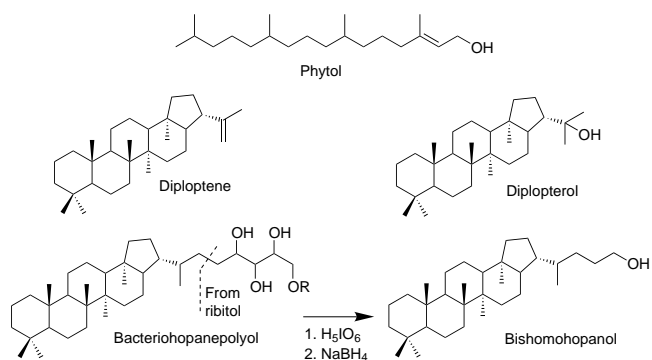


**Figure 31.** Polyisoprenoids produced by *Synechocystis* sp. and analyzed isotopically by Sakata *et al.* (1997). The bacteriohopanepolyol is too polar to be isolated in good yield. As is common in such cases, the procedure introduced by Rohmer *et al.* (1984) was therefore applied, with periodic acid being used to cleave the bonds between OH-bearing carbon atoms. Treatment with sodium borohydride then produces a C<sub>32</sub> alcohol that can be recovered in good yield for further studies.

dance of bacteriohopanepolyol was more strongly correlated with cellular volume (Jürgens *et al.*, 1992), Sakata *et al.* (1997) attributed the difference to changing branching ratios over the life of the cell, with greater depletion being favored in the later (volume-correlated) products.

The results provide some information about the isotopic characteristics of the MEP pathway of isoprenoid biosynthesis. As shown in Figure 29, there are two processes by which MEP might be depleted in <sup>13</sup>C relative to photosynthate. The first is in the decarboxylation of pyruvate to yield the C<sub>2</sub> unit which is condensed with glyceraldehyde to yield deoxyxylulose. The second – if, as seems likely for a C<sub>5</sub> carbohydrate, the deoxyxylulose has alternate fates – is in the rearrangement of the linear carbon skeleton to yield methylerythritol. If only the first of these steps were effective, only the tertiary C would be depleted in each isoprene unit and, to account for the observed overall depletion of 6.8‰, the depletion at that position would be 34‰. Since this exceeds the isotope effect found or estimated for any enzyme-catalyzed decarboxylation of pyruvate, it appears very likely that further fractionation, affecting at least one if not two additional carbon positions, is associated with the second step.

### A survey of carbon isotopic compositions of lipids from other organisms

The lipid fractionations discussed in the preceding paragraphs provide the first entries in Table 5, which also summarizes results from many further investigations and provides a basis for discussion.

Lipids from several photosynthetic bacteria have been studied (photosynthetic bacteria are anaerobic phototrophs that use electron donors other than water and which are distinct from cyanobacteria). The Chromatiaceae (*Chromatium*, *Thiocapsa*) can grow photoheterotrophically (using light energy but an organic carbon source) as well as

Table 5. Observed depletions of  $^{13}\text{C}$  in lipids relative to biomass, prokaryotes

Organism <sup>a</sup>	C source	Metabolism	$\delta\text{Biomass/Lipid, } \text{‰}$		Reference
			<i>n</i> -Alkyl	Isopren. <sup>b</sup>	
<i>E. coli</i>	glucose	het. O <sub>2</sub>	3		Monson and Hayes, 1982
<i>E. coli</i>	glucose	het. O <sub>2</sub>	3		Blair <i>et al.</i> , 1985
<i>S. putrefaciens</i>	lactate	het. O <sub>2</sub>	2-3		Teece <i>et al.</i> , 1999
<i>S. putrefaciens</i>	lactate	het. NO <sub>3</sub> <sup>-</sup>	5-10		Teece <i>et al.</i> , 1999
<i>Synechocystis</i> sp.	CO <sub>2</sub>	C <sub>3</sub>	9	6-8 E	Sakata <i>et al.</i> , 1997
<i>C. tepidum</i>	CO <sub>2</sub>	C <sub>3</sub>		3.5 E	Madigan <i>et al.</i> , 1989
<i>C. tepidum</i>	acetate	photohet.		5 E	Madigan <i>et al.</i> , 1989
<i>C. vinosum</i>	CO <sub>2</sub>	C <sub>3</sub>		4.1 E	Takigiku, 1987
<i>Rps. capsulata</i>	CO <sub>2</sub>	C <sub>3</sub>		4.9 E	Takigiku, 1987
<i>C. limicola</i>	CO <sub>2</sub>	rev. TCA	-16 - -11 <sup>c</sup>	-2 - -3 E	van der Meer <i>et al.</i> , 1998
<i>T. roseopersicina</i>	CO <sub>2</sub>	C <sub>3</sub> + rev. TCA	-4 - 2 <sup>d</sup>	4-5 E	van der Meer <i>et al.</i> , 1998
<i>C. aurantiacus</i>	CO <sub>2</sub>	3-OH prop.	0.7	4 V	van der Meer <i>et al.</i> , 2001b
<i>Rhodospirillum rubrum</i>	CO <sub>2</sub>	C <sub>3</sub> NH <sub>3</sub> /O <sub>2</sub>	7-13	9.3 E	Sakata <i>et al.</i> , 2001
<i>N. europaea</i>	CO <sub>2</sub>	unknown	-2		Jahnke <i>et al.</i> , 2001
<i>M. capsulatus</i>	CH <sub>4</sub>	RuMP	2-4	6-11 <sup>e</sup> E	Summons <i>et al.</i> , 1994
<i>M. capsulatus</i>	CH <sub>4</sub>	RuMP	2-4	6-10 E	Jahnke <i>et al.</i> , 1999
<i>M. trichosporium</i>	CH <sub>4</sub>	serine	12	2 E	Jahnke <i>et al.</i> , 1999
CEL 1923	CH <sub>4</sub>	RuMP	5	6.4 E	Jahnke <i>et al.</i> , 1999
<i>M. barkeri</i>	N(CH <sub>3</sub> ) <sub>3</sub>	M'gen		18 V	Summons <i>et al.</i> , 1998
<i>M. burtonii</i>	N(CH <sub>3</sub> ) <sub>3</sub>	M'gen		29 V	Summons <i>et al.</i> , 1998
<i>M. thermoautotrophicum</i>	CO <sub>2</sub>	M'gen		13 V	Takigiku, 1987
<i>M. sedula</i>	CO <sub>2</sub>	3-OH prop.		-2	van der Meer <i>et al.</i> , 2001a

-----  
<sup>a</sup> For genera see text. <sup>b</sup> E = MEP, V = MVA. <sup>c</sup> 17:1 unique at -5‰. <sup>d</sup> 17:0 unique at 4‰. <sup>e</sup> Tabulated depletions pertain only to end products formed early in life of a culture, when only the membrane-bound form of methane monooxygenase (MMO) is present. Squalene is enriched relative to end products. Fractionations decrease when soluble MMO is also present.

629). Van der Meer *et al.* (1998) note that the inverse fractionation (= enrichment) of  $^{13}\text{C}$  in *n*-alkyl carbon skeletons produced by *T. roseopersicina* may be due to use of acetate produced by the reversed TCA cycle (see discussion of *C. limicola*, below).

Chemoautotrophs are microbes which obtain energy by catalyzing an exergonic chemical reaction (commonly at interfaces between aerobic and anaerobic environments) and which produce biomass by fixing inorganic carbon. *Nitrosomonas europaea* oxidizes ammonia and uses rubisco and the Calvin Cycle to fix carbon (the most common sulfide-oxidizing organisms also use the Calvin Cycle). Its isotopic characteristics could therefore, be expected to be similar to those of other aerobic, prokaryotic autotrophs such as *Synechocystis*. As shown in Table 5, this expectation is fulfilled.

Nearly all of the remaining organisms listed in Table 5 do not produce C<sub>3</sub>–C<sub>6</sub> carbohydrates as immediate products of carbon fixation nor do they commonly assimilate them (*M. capsulatus* is the exception). As a result, pathways of carbon flow differ strongly from those in the organisms already discussed. *Chlorobium limicola*, for example, is a member of the Chlorobiaceae, which use the

reversed TCA Cycle for fixation of carbon. Van der Meer *et al.* (1998) point out that the flow of carbon in such organisms proceeds from CO<sub>2</sub> to acetate and then to C<sub>3</sub> and larger compounds. Since each further step brings a chance for more fractionation, it should not be surprising that *n*-alkyl carbon skeletons are enriched in  $^{13}\text{C}$  relative to biomass, although the magnitude of the enrichment in comparison to that observed in isoprenoids is both remarkable and unexplained.

*Chloroflexus aurantiacus* fixes carbon using the 3-hydroxypropionate pathway (Strauss and Fuchs, 1993). Remarkably, it is known also to produce its isoprenoids from acetate via the MVA pathway (Rieder *et al.*, 1998). Van der Meer *et al.* (2001b) point out that, if the same pool of acetate is used to produce the *n*-alkyl lipids, the isotopic compositions at the methyl and carboxyl positions of the acetate groups used in biosynthesis can be calculated (e. g., there are 12 methyl and 8 carboxyl carbons in the C<sub>20</sub> isoprenoid and 8 of each in the C<sub>16</sub> fatty acid). The fractionations reported in Table 5 then indicate that the carboxyl carbon is enriched in  $^{13}\text{C}$  relative to the methyl carbon by 40‰! The pathways of carbon flow in *C. aurantiacus* are very incompletely known and the branch points poten-

tially responsible for such a large fractionation cannot be identified.

*Thermocrinus ruber* is a hyperthermophilic, hydrogen-oxidizing chemoautotroph. The pathway by which it assimilates inorganic carbon is unknown. Its biomass is depleted relative to CO<sub>2</sub> by only 3‰. The *n*-alkyl lipids are in turn slightly enriched relative to biomass so that their isotopic composition is very close to that of the CO<sub>2</sub>. In this case, fractionations may be minimized both by the high temperature, which reduces the magnitude of equilibrium isotope effects, and by the structure of the metabolic reaction network, which apparently leads to similar isotopic compositions for the precursors of both amino acids and lipids.

The remaining entries in Table 5 are involved in the production and consumption of methane. *Methylococcus capsulatus*, *Methylosinus trichosporium*, and the isolate designated as CEL1923 are methylotrophic bacteria. Such organisms assimilate methane (and, in many cases, other “C<sub>1</sub> compounds,” such as methanol, formaldehyde, formic acid, methyl amines, and methyl sulfides) using either a pathway that yields carbohydrates (the ribulose monophosphate or RuMP pathway) or one which yields acetyl-CoA after the C<sub>1</sub> unit is initially added to glycine to yield serine (thus called the serine pathway). The methyl carbon in that acetyl-CoA derives from the C<sub>1</sub> substrate but the carboxyl carbon derives from CO<sub>2</sub>. Variations are possible within the serine pathway. 3-Phosphoglyceric acid, an oxidation product of serine, can be withdrawn from the pathway much as C<sub>4</sub> and C<sub>5</sub> acids are withdrawn from the TCA cycle (Jahnke *et al.*, 1999). The acetyl-CoA product can reenter the cycle and lead to the production of succinate for use in biosyntheses (White, 1995, p. 265).

The RuMP- and serine-pathway methylotrophs yield sharply contrasting lipid-biosynthetic fractionations. In *M. capsulatus*, the *n*-alkyl carbon skeletons are depleted by 2-4‰ and the isoprenoids are depleted by 6-11‰. This resembles patterns seen in other prokaryotes in which biosynthesis starts from carbohydrates. The *n*-alkyl carbon skeletons are depleted as in *E. coli* and the isoprenoids are depleted roughly as in *Synechocystis* and *N. europea*. But *M. capsulatus* does not have a complete TCA cycle. Processes unique to the RuMP-cycle methylotrophs must be controlling the isotopic compositions of the lipid precursors in *M. capsulatus*. The serine pathway used by *M. trichosporium* leads straightforwardly to acetyl-CoA but not to building blocks for isoprene units. Why, then, are the *n*-alkyl carbon skeletons from serine-cycle methanotrophs so much more strongly depleted than the isoprenoids? If phosphoglyceric acid is withdrawn from the pathway and condensed with a C<sub>2</sub> unit to obtain deoxyxylulose, where is that C<sub>2</sub> unit coming from? It cannot be the same acetyl-CoA that is yielding the strongly depleted *n*-alkyl carbon skeletons. Very interestingly, the strong depletion in the *n*-alkyl carbon skeletons resembles that in anaerobic cultures of *Shewanella*, in which serine-pathway metabolism has

been invoked on the basis of enzymological studies (Scott and Nealson, 1994).

The initial study of *M. capsulatus* (Summons *et al.*, 1994) provided the best example of temporal variations in isotopic fractionations. Two variants of methane monooxygenase, one soluble, the other membrane-bound, mediate the assimilation of methane. The membrane-bound enzyme is dominant at low cell densities (*i. e.*, during the exponential phase of growth) and has an isotope effect that is large compared to that of the soluble enzyme, which becomes important later. As a result, all of the carbon initially available for production of biomass is depleted in <sup>13</sup>C relative to that assimilated later. The mixture of lipids produced also changes as the culture ages. Specifically, 3-methyl bacteriohopanepolyol and 4,4-dimethylsterols increase in abundance relative to bacteriohopanepolyol and 4-methyl sterols. As a result of these changes, the late-synthesized methyl hopanoids and dimethyl sterols are enriched in <sup>13</sup>C relative to the nonmethylated hopanoids and monomethyl sterols even though all derive from the same precursor (namely, squalene). The effect could be observed only by harvesting cultures at varying cell densities and making repeated analyses, and that very laborious task was undertaken only after initial observations (based, of course, on large amounts of material from fully grown cultures) had yielded “impossible” results (*e. g.*, monomethyl sterols strongly depleted in <sup>13</sup>C relative to their dimethyl homologs). These elegant investigations also showed the squalene itself was commonly enriched in <sup>13</sup>C by 5-7‰ relative to its products, indicating that an isotope effect significant even for a 30-carbon molecule must be associated with the cyclization reaction.

Individual lipids have been isotopically analyzed in only three Archaea, all of them methanogens (see entries for *Methanosarcina barkeri*, *Methanococcoides burtonii*, and *Methanobacterium thermoautotrophicum* in Table 5). All reflect strong depletion of <sup>13</sup>C in lipids relative to biomass. Methanogens are commonly described as fixing carbon by use of the acetyl-CoA pathway. This can provide the feedstock required for synthesis of lipids, but C<sub>3</sub> and C<sub>4</sub> carbon skeletons are required for the synthesis of amino acids (which, in the form of proteins, account for most of the biomass). In methanogens, these are produced by additional CO<sub>2</sub>-fixing steps (White, 1995, p. 261). If the isotope effects associated with those reactions are much smaller than those associated with the production of acetyl-CoA, the isotopic contrast between the lipids and the biomass can be accounted for.

The entries in Table 6 pertain to eukaryotic algae. *S. communis*, *T. minimum*, *C. monoica*, and *Dunaliella* sp. are green algae and are expected to synthesize isoprenoids *via* the MEP pathway in the cytosol as well as in the plastids. The remaining species are expected to utilize the MEP pathway within the chloroplast and the MVA pathway in the cytosol. By far the most thorough and precise investigation was that of biosynthesis in *E. huxleyii* undertaken

by Riebesell *et al.* (2000). Their analyses resolved four lipid groups: phytol and the C<sub>14</sub> and C<sub>16</sub> fatty acids, all depleted relative to biomass by 2 - 2.5‰ in spite of their contrasting origins from acetyl-CoA and methyerythritol; the unsaturated C<sub>18</sub> fatty acids and a C<sub>36</sub> alkadiene (apparently produced from two C<sub>18</sub> acid skeletons), all depleted by 4‰; the C<sub>37</sub> and C<sub>38</sub> alkenones, depleted by 5.2‰; and a dominant sterol depleted by 8.3‰. Comfort can be taken from the fact that the other entry that comes closest to duplicating this pattern refers to additional analyses of *E. huxleyi*.

Depletions of <sup>13</sup>C in the C<sub>37</sub> alkenones produced by *E. huxleyi* are of particular interest and illustrate a key point. The abundances of the alkenones relative to other products vary substantially depending on conditions of growth. For example, Riebesell *et al.* (2000) found that the alkenones comprised 1.0% of biomass C at low concentrations of dissolved CO<sub>2</sub> and up to 5.9% of biomass C at higher concentrations of dissolved CO<sub>2</sub>. In spite of this variation in abundance, the depletion of <sup>13</sup>C relative to biomass in the C<sub>37</sub> alkadiene consistently averaged 5.4‰ (s. d. = 0.3‰, n = 10) and was not correlated with [CO<sub>2</sub>(aq)]. If, on the other hand, the isotopic composition of the same compound was expressed relative to that of the fully saturated C<sub>16</sub> fatty acid it varied systematically from a depletion of 2.5‰ at low concentrations of dissolved CO<sub>2</sub> to a depletion of 4.0‰ at high concentrations, apparently reflecting a progressive redistribution of carbon within the lipid-biosynthetic reaction network. Although they found a significantly different fractionation (4.2 vs. 5.4‰, light and nutrient limitations varied between the two treatments), Popp *et al.* (1998a) found that the isotopic composition of the C<sub>37</sub> alkadiene relative to biomass did not vary systematically with rate of growth although the isotopic composition of the biomass relative to the source CO<sub>2</sub> varied strongly.

Patterns of isotopic depletion among compound classes for other species frequently differ. It appears common, but far from universal, for MVA-pathway sterols to be depleted relative to biomass by 5-8‰. Phytol is nearly always less strongly depleted (2-5.5‰). Both of these relationships are consistent with field data summarized by Popp *et al.* (1999). If extended (≥ C<sub>18</sub>) *n*-alkyl carbon skeletons are abundant, they are often isotopically depleted relative to the C<sub>14</sub>-C<sub>17</sub> fatty acids. Differences of more than about 1‰ cannot reasonably be attributed to the addition of a single, isotopically exotic acetyl unit (*i. e.*, during the extension of a C<sub>16</sub> chain to C<sub>18</sub>). Such contrasts, therefore, probably indicate the use of distinct pools of acetate. There is a problem, however, in asserting that the lighter *n*-alkyl carbon skeletons must derive from cytosolic acetate, since the MVA-derived isoprenoids must also come from that pool

Table 6. Observed depletions of <sup>13</sup>C in lipids relative to biomass, eukaryotic algae

Organism	$\epsilon_{\text{Biomass/Lipid}}$ , ‰		Reference
	<i>n</i> -Alkyl <sup>a</sup>	Isoprenoids <sup>b</sup>	
<i>Scenedesmus communis</i>	7-9, 12	5.3 Ep, 7 Ec	Schouten <i>et al.</i> , 1998
<i>Tetraedron minimum</i>	3-6, 6	0-5 Ep, -2 Ec	Schouten <i>et al.</i> , 1998
<i>Chlamydomonas monoica</i>	7.5	4.9 Ep, 5.1 Ec	Schouten <i>et al.</i> , 1998
<i>Dunaliella</i> sp.	3.5	0.5 Ep, -2.7 Ec	Schouten <i>et al.</i> , 1998
<i>Rhizosolenia setigera</i>	5-7	2.9 Ep, 6-7 Vc	Schouten <i>et al.</i> , 1998
<i>Chaetoceros socialis</i>	0-2	-1 Ep	Schouten <i>et al.</i> , 1998
<i>Thalassiosira weissflogii</i>	1-2	1 Vc	Schouten <i>et al.</i> , 1998
<i>Gymnodinium simplex</i>	1-3	4.5 Vc	Schouten <i>et al.</i> , 1998
<i>Isochrysis galbana</i>	6-8, 3.1	2.8 Ep, 7 Vc	Schouten <i>et al.</i> , 1998
<i>Chrysochromulina polylepis</i>	6	2.7 Ep	Schouten <i>et al.</i> , 1998
<i>Tetraselmis</i> sp.	8	4.2 Ep, 0.4 Ec	Schouten <i>et al.</i> , 1998
<i>Rhodomonas</i> sp.	5-7	2.2 Ep, 1 Vc	Schouten <i>et al.</i> , 1998
<i>Phaeodactylum tricorutum</i>	9, 7	3.4 Ep, 7.2 Vc	Bidigare <i>et al.</i> , 1997
<i>Emiliania huxleyi</i>	6, 4.1	4.2 Ep, 7.3 Vc	Bidigare <i>et al.</i> , 1997
<i>Emiliania huxleyi</i>	4.2 <sup>c</sup>		Popp <i>et al.</i> , 1998a
<i>Emiliania huxleyi</i>	2.5, 4.0, 5.4 <sup>d</sup>	2.0 Ep, 8.3 Vc	Riebesell <i>et al.</i> , 2000

<sup>a</sup> In multiple entries, the first number or range pertains to C<sub>14</sub>-C<sub>18</sub> carbon skeletons presumably of plastidic origin and the second pertains to extended chains that may be of cytosolic origin. <sup>b</sup> E, MEP pathway; V, MVA pathway; p, plastid; c, cytosol. <sup>c</sup> C<sub>37</sub> alkadiene only. <sup>d</sup> In sequence: C<sub>14</sub> and C<sub>16</sub> fatty acids, C<sub>18</sub> and C<sub>36</sub> fatty acids, C<sub>22</sub> fatty acid + C<sub>37</sub> and C<sub>38</sub> alkenones.

and they are generally lighter still. To explore these relationships more securely, some immediate objectives can be defined. We need to determine how much of the variability evident among the eukaryotic algae is experimental (analytical noise, stressed cultures under unnatural conditions, *etc.*) and how much is biological (response to subtle factors that may well vary in natural environments). We need to obtain a better view of the comparative isotopic characteristics of the MEP and MVA pathways. More analyses of sterols from green algae and *any* analyses of products of *Euglena* (in which the MVA pathway is found in both the plastid and the cytosol) would be helpful.

## Epilogue

It often seems that isotopic fractionations provide *too much* information about *too many* processes, combining it all in a package that is unmanageably intricate. In response, investigators keep increasing the complexity of the available data by providing more and more detailed analyses. The proliferation of compound-specific isotopic analyses is a prime example of this phenomenon. Does it increase the information-carrying capacity of the isotopic channel or is it another case of the triumph of entropy? To obtain the preferred result, we will have to understand biosynthetic fractionations like those reviewed here.

## Acknowledgements

Support for this work and for the author's molecular-isotopic studies in general has come from the Programs in Exobiology and in Astrobiology at the National Aeronautics and Space Administration. It is a privilege also to acknowledge advice, comments, manuscripts, and reviews provided by Bob Bidigare, Marilyn Fogel, Ed Laws, Alex Sessions, Roger Summons, and Marcel van der Meer.

## References

- Abelson PH, Hoering TC (1961) Carbon isotope fractionation in formation of amino acids by photosynthetic organisms. *Proc NAS* 47:623-632
- Anderson LA (1995) On the hydrogen and oxygen content of marine phytoplankton. *Deep-Sea Research* 42:1675-1680
- Belyaev SS, Wolkin R, Kenealy WR, DeNiro MJ, Epstein S, Zeikus JG (1983) Methanogenic bacteria from the Bondyuzhskoe oil field: general characterization and analysis of stable-carbon isotopic fractionation. *Appl Environ Microbiol* 45:691-697
- Benner R, Fogel ML, Sprague EK, Hodson RE (1987) Depletion of  $^{13}\text{C}$  in lignin and its implications for stable carbon isotope studies. *Nature* 329:708-710
- Bidigare RR, Hanson KL, Buesseler KO, Wakeham SG, Freeman KH, Pancost RD, Millero FJ, Steinberg P, Popp BN, Latasa M, Landry MR, Laws EA (1999) Iron-stimulated changes in  $^{13}\text{C}$  fractionation and export by equatorial Pacific phytoplankton: toward a paleogrowth rate proxy. *Paleoceanography* 14:589-595
- Bidigare RR, Popp BN, Kenig F, Hanson K, Laws EA, Wakeham SG (1997) Variations in the stable carbon isotopic composition of algal biomarkers. Abstracts, 18th International Meeting on Organic Geochemistry 22-26 September, Maastricht, The Netherlands p. 119-120
- Bird CW, Lynch JM, Pirt FJ, Reid WW, Brooks CJW, Middleditch BS (1971) Steroids and squalene in *Methylococcus capsulatus* grown on methane. *Nature* 230:473-474
- Blair N, Leu A, Muñoz E, Olsen J, Des Marais D (1985) Carbon isotopic fractionation in heterotrophic microbial metabolism. *Appl Environ Microbiol* 50:996-1001
- Boucher Y, Doolittle WF (2000) The role of lateral gene transfer in the evolution of isoprenoid biosynthesis pathways. *Mol Microbiol* 37:703-716
- Calvin M, Bascham JA (1962) The photosynthesis of carbon compounds. WA Benjamin, New York
- Cavalier-Smith T (2000) Membrane heredity and early chloroplast evolution. *Trends Plant Sci* 5:174-182
- Cleland WW, O'Leary MH, Northrop DB (eds) (1977) Isotope Effects on Enzyme-Catalyzed Reactions. Appendix A: A note on the Use of Fractionation Factors versus Isotope Effects on Rate Constants. University Park Press, Baltimore, Maryland
- Coffin RB, Velinsky DJ, Devereux R, Price WA, Cifuentes LA (1990) Stable carbon isotope analysis of nucleic acids to trace sources of dissolved substrates used by estuarine bacteria. *Appl Environ Microbiol* 56:2012-2020
- Coffin RB, Cifuentes LA, Elderidge PM (1994) The use of stable carbon isotopes to study microbial processes in estuaries. In: K Lajtha, RH Michener (eds) *Stable Isotopes in Ecology and Environmental Science* p 222-240 Blackwell Scientific Publications, Oxford, England
- Coffin RB, Cifuentes LA, Pritchard PH (1997) Assimilation of oil-derived carbon and remedial nitrogen applications by intertidal food chains on a contaminated beach in Prince William Sound, Alaska. *Mar Environ Res* 44:27-39
- Cronan JE, Vagelos PR (1972) Metabolism and function of the membrane phospholipids of *Escherichia coli*. *Biochimica et Biophysica Acta* 265: 25-60
- DeNiro MJ, Epstein S (1977) Mechanism of carbon isotope fractionation associated with lipid synthesis. *Science* 197:261-263
- Descolas-Gros C, Fontugne M (1990) Stable carbon isotope fractionation by marine phytoplankton during photosynthesis. *Plant, Cell and Environment* 13:207-218
- Disch A, Schwender J, Müller C, Lichtenthaler HK, Rohmer M (1998) Distribution of the mevalonate and glyceraldehyde phosphate/pyruvate pathways for isoprenoid biosynthesis in unicellular algae and the cyanobacterium *Synechocystis* PCC 6714. *Biochem J* 333:381-388
- Estep MF, Hoering TC (1980) Biogeochemistry of the stable hydrogen isotopes. *Geochim Cosmochim Acta* 44:1197-1206
- Falkowski PG, Raven JA (1997) Aquatic Photosynthesis. Blackwell Science, Massachusetts
- Farquhar GD (1983) On the nature of carbon isotope discrimination in  $\text{C}_4$  species. *Aust J Plant Physiol* 10:205-226
- Farquhar GD, Ehleringer JR, Hubick KT (1989) Carbon isotope discrimination and photosynthesis. *Annu Rev Plant Physiol Plant Mol Biol* 40:503-537
- Flesch G, Rohmer M (1988) Prokaryotic hopanoids: the biosynthesis of the bacteriohopane skeleton. *Eur J Biochem* 175:405-411
- Fogel ML, Tuross N (1999) Transformation of plant biochemicals to geological macromolecules during early diagenesis. *Oecologia* 120:336-346
- Garrett RH, Grisham CM (1999) Biochemistry, second edition. Harcourt College Publishers, Philadelphia, Pennsylvania
- Gelwicks JT, Risatti JB, Hayes JM (1989) Carbon isotope effects associated with autotrophic acetogenesis. *Org*

Geochem 14:441-446

Guy RD, Fogel ML, Berry JA (1993) Photosynthetic fractionation of the stable isotopes of oxygen and carbon. *Plant Physiol* 101:37-47

Hatch MD (1977) C<sub>4</sub> pathway of photosynthesis: mechanism and physiological function. *Trends in Biochemical Sciences* 2:199-202

Hare PE, Fogel ML, Stafford Jr. TW, Mitchell AD, Hoering TC (1991) The isotopic composition of carbon and nitrogen in individual amino acids isolated from modern and fossil proteins. *J Archaeol Sci* 18:277-292

Hayes JH (2000) Lipids as a common interest of microorganisms and geochemists. *PNAS* 97:14033-14034

Ivanovsky RN (1985) Carbon metabolism in phototrophic bacteria under different conditions of growth. In: IS Kulaev, EA Dawes, DW Tempest (eds) *Environmental Regulation of Microbial Metabolism*, FEMS Symposium No. 23, p 263-272 Academic Press, New York

Jähne B, Heinz G, Dietrich W (1987) Measurement of the diffusion coefficients of sparingly soluble gases in water. *J Geophys Res* 92:10,767-10,10,776

Jahnke LL, Summons RE, Hope JM, Des Marais DJ (1999) Carbon isotopic fractionation in lipids from methanotrophic bacteria II: The effects of physiology and environmental parameters on the biosynthesis and isotopic signatures of biomarkers. *Geochim Cosmochim Acta* 63:79-93

Jahnke LL, Summons RE, Hope JM, Eder W, Huber R, Stetter KO, Hinrichs K-U, Hayes JH, Des Marais DJ, Cady S (2001) Composition of hydrothermal vent microbial communities as revealed by analyses of signature lipids, stable carbon isotopes and *Aquificales* cultures. Submitted to *Appl Env Microbiol*

Jürgens UJ, Simonin P, Rohmer M (1992) Localization and distribution of hopanoids in membrane systems of the cyanobacterium *Synechocystis* PCC6714. *FEMS Microbiol Lett* 92:285-288

Keil RG, Fogel ML (2001) Reworking of amino acid in marine sediments: Stable carbon isotopic composition of amino acids in sediments along the Washington coast. *Limnol Oceanogr* 46:14-23

Kleemann G, Poralla K, Englert G, Kjösen H, Liaaen-Jensen S, Neunlist S, Rohmer M (1990) Tetrahymanol from the phototrophic bacterium *Rhodospseudomonas palustris*: first report of a gammacerane triterpene from a prokaryote. *J Gen Microbiol* 136:2551-2553

Kleinig H (1989) The role of plastids in isoprenoid biosynthesis. *Annu Rev Plant Physiol Plant Mol Biol* 40:39-59

Kohl W, Gloe A, Reichenbach H (1983) Steroids from the Myxobacterium *Nannocystis exedens*. *J Gen Microbiol* 129:1629-1635

Lange BM, Rujan T, Martin W, Croteau R (2000) Iso-

prenoid biosynthesis: The evolution of two ancient and distinct pathways across genomes. *PNAS* 97:13172-13177

Laws EA (1991) Photosynthetic quotients, new production and net community production in the open ocean. *Deep-Sea Research* 38:143-167

Laws EA, Popp BN, Bidigare RR, Kennicutt MC, Macko SA (1995) Dependence of phytoplankton carbon isotopic composition on growth rate and [CO<sub>2</sub>]<sub>aq</sub>: Theoretical considerations and experimental results. *Geochim Cosmochim Acta* 59:1131-1138

Levin EY, Bloch K (1964) Absence of sterols in blue-green algae. *Nature* 202:90-91

Lichtenthaler HK, Schwender J, Disch A, Rohmer M (1997) Biosynthesis of isoprenoids in higher plant chloroplasts proceeds via a mevalonate-independent pathway. *FEBS Letters* 400:271-274

Lichtenthaler HK (1999) The 1-deoxy-D-xylulose-5-phosphate pathway of isoprenoid biosynthesis in plants. *Annu Rev Plant Physiol Plant Mol Biol* 50:47-65

Luo Y, Sternberg L (1991) Deuterium heterogeneity in starch and cellulose nitrate of CAM and C<sub>3</sub> plants. *Phytochemistry* 30:1095-1098

Luo Y-H, Sternberg L, Suda S, Kumazawa S, Mitsui A (1991) Extremely low D/H ratios of photoproduced hydrogen by cyanobacteria. *Plant Cell Physiol* 32:897-900

Macko SA, Fogel ML, Hare PE, Hoering TC (1987) Isotopic fractionation of nitrogen and carbon in the synthesis of amino acids by microorganisms. *Chem Geol* 65:79-92

Madigan MT, Takigiku R, Lee RG, Gest H, Hayes JM (1989) Carbon isotope fractionation by thermophilic phototrophic sulfur bacteria: Evidence for autotrophic growth in natural populations. *Appl Env Microbiol* 55:639-644

Madigan MT, Martinko JM, Parker J (2000) *Brock Biology of Microorganisms*, ninth edition. Prentice Hall, New Jersey

Marino BD, McElroy MB (1991) Isotopic composition of atmospheric CO<sub>2</sub> inferred from carbon in C<sub>4</sub> plant cellulose. *Nature* 349:127-131

Melzer E, Schmidt H-L (1987) Carbon isotope effects on the pyruvate dehydrogenase reaction and their importance for relative carbon-13 depletion in lipids. *J Biol Chem* 262:8159-8164

Melzer E, O'Leary MH (1987) Anapleurotic CO<sub>2</sub> fixation by phosphoenolpyruvate carboxylase in C<sub>3</sub> plants. *Plant Physiol* 84:58-60

Melzer E, O'Leary MH (1991) Aspartic-acid synthesis in C<sub>3</sub> plants. *Planta* 185:368-371

Monson KD, Hayes JM (1980) Biosynthetic control of the natural abundance of carbon 13 at specific positions within fatty acids in *Escherichia coli*. *J Biol Chem* 255:11435-11441

- Monson KD, Hayes JM (1982a) Carbon isotopic fractionation in the biosynthesis of bacterial fatty acids. Ozonolysis of unsaturated fatty acids as a means of determining the intramolecular distribution of carbon isotopes. *Geochim Cosmochim Acta* 46:139-149
- Monson KD, Hayes JM (1982b) Biosynthetic control of the natural abundance of carbon 13 at specific position within fatty acids in *Saccharomyces cerevisiae*. Isotope fractionations in lipid synthesis as evidence for peroxisomal regulation. *J Biol Chem* 257: 5568-5575
- Mook WG, Bommerson JC, Staverman MH (1974) Carbon isotope fractionation between dissolved bicarbonate and gaseous carbon dioxide. *Earth Planet Sci Lett* 22:169-175
- Moore S, Stein WH (1951) Chromatography of amino acids on sulfonated polystyrene resins. *J Biol Chem* 192:663-681
- Ohlrogge JB, Jaworski JG (1997) Regulation of fatty acid synthesis. *Annu Rev Plant Physiol Plant Mol Biol* 48:109-136
- O'Leary MH (1981) Carbon isotope fractionation in plants. *Phytochemistry* 20:553-567
- O'Leary MH, Rife JE, Slater JD (1981) Kinetic and isotope effect studies of maize phosphoenolpyruvate carboxylase. *Biochemistry* 20:7308-7314
- O'Leary MH (1984) Measurement of the isotope fractionation associated with diffusion of carbon dioxide in aqueous solution. *J Phys Chem* 88:823-825
- Popp BN, Kenig F, Wakeham SG, Laws EA, Bidigare RR (1998a) Does growth rate affect ketone unsaturation and intracellular carbon isotopic variability in *Emiliania huxleyi*? *Paleoceanography* 13:35-41
- Popp BN, Laws EA, Bidigare RR, Dore JE, Hanson KL, Wakeham SG (1998b) Effect of phytoplankton cell geometry on carbon isotopic fractionation. *Geochim Cosmochim Acta* 62:69-77
- Popp BN, Trull T, Kenig F, Wakeham SG, Rust TM, Tilbrook B, Griffiths FB, Wright SW, Marchant HJ, Bidigare RR, Laws EA (1999) Controls on the carbon isotopic composition of Southern Ocean phytoplankton. *Global Biogeochem Cycles* 13:827-843
- Preub A, Schauder R, Fuchs G, Stichler W (1989) Carbon isotope fractionation by autotrophic bacteria with three different CO<sub>2</sub> fixation pathways. *Z Naturforsch* 44:397-402
- Raederstorff D, Rohmer M (1988) Polyterpenoids as cholesterol and tetrahymanol surrogates in the ciliate *Tetrahymana pyriformis*. *Biochimica et Biophysica Acta* 960:190-199
- Razin S (1978) The mycoplasmas. *Microbiol Rev* 42:414-470
- Reinfelder JR, Kraepiel AML, Morel FMM (2000) Unicellular C<sub>4</sub> photosynthesis in a marine diatom. *Nature* 407:996-999
- Riebesell U, Revill AT, Holdsworth DG, Volkman JK (2000) The effects of varying CO<sub>2</sub> concentration on lipid composition and carbon isotope fractionation in *Emiliania huxleyi*. *Geochim Cosmochim Acta* 64:4179-4192
- Rieder C, Straub G, Fuchs G, Arigoni D, Bacher A, Eisenreich W (1998) Biosynthesis of the diterpene verrucosan-2b-ol in the phototrophic eubacterium *Chloroflexus aurantiacus*. *J Biol Chem* 273:18099-18108
- Roberts RB, Abelson PH, Cowie DB, Bolton ET, Britten RJ (1955) Studies of biosynthesis in *Escherichia coli*. Carnegie Institution of Washington Publication 607, Washington, D.C.
- Robinson JJ, Cavanaugh CM (1995) Expression of form I and form II Rubisco in chemoautotrophic symbioses: Implications for the interpretation of stable carbon isotope values. *Limnol Oceanogr* 40:1496-1502
- Roeske CA, O'Leary MH (1984) Carbon isotope effects on the enzyme-catalyzed carboxylation of ribulose biphosphate. *Biochemistry* 23:6275-6284
- Roeske CA, O'Leary MH (1985) Carbon isotope effect on carboxylation of ribulose biphosphate catalyzed by ribulosebiphosphate carboxylase from *Rhodospirillum rubrum*. *Biochemistry* 24:1603-1607
- Rohmer M, Bouvier-Nave P, Ourisson G (1984) Distribution of hopanoid triterpenes in prokaryotes. *J Gen Microbiol* 130:1137-1150
- Rohmer M (1993) The biosynthesis of triterpenoids of the hopane series in the Eubacteria: A mine of new enzyme reactions. *Pure and Appl Chem* 65:1293-1298
- Rohmer M, Knani M, Simonin P, Sutter B, Sahn H (1993) Isoprenoid biosynthesis in bacteria: a novel pathway for the early steps leading to isopentenyl diphosphate. *Biochem J* 295:517-524
- Rossmann A, Butzenlechner M, Schmidt H-L (1991) Evidence for a nonstatistical carbon isotope distribution in natural glucose. *Plant Physiol* 96:609-614
- Rowland SJ, Belt ST, Cooke DA, Hird SJ, Neeley S, Robert J-M (1995) Structural characterisation of saturated through heptaunsaturated C<sub>25</sub> highly branched isoprenoids. In: JO Grimalt, C Dorronsoro (eds) *Organic Geochemistry: Developments and Applications to Energy, Climate, Environment and Human History*, p 581-582 A.I.G.O.A., The Basque Country, Spain
- Sakata S, Hayes JH, McTaggart AR, Evans RA, Leckrone KJ, Togasaki RK (1997) Carbon isotopic fractionation associated with lipid biosynthesis by a cyanobacterium: Relevance for interpretation of biomarker records. *Geochim Cosmochim Acta* 61:5379-5389
- Sakata S, Hayes JH, Rohmer M, Hooper AB, Seeman M (2001) Molecular and carbon isotopic compositions of

lipids isolated from an ammonia-oxidizing chemoautotroph. Submitted to Proc Nat Acad Sci USA

Schleucher J, Vanderveer PJ, Sharkey TD (1998) Export of carbon from chloroplasts at night. *Plant Physiol* 118:1439-1445

Schouten S, Klein Breteler WCM, Blokker P, Schogt N, Rijpstra WIC, Grice K, Baas M, Sinninghe Damasté JS (1998) Biosynthetic effects on the stable carbon isotopic compositions of algal lipids: Implications for deciphering the carbon isotopic biomarker record. *Geochim Cosmochim Acta* 62:1397-1406

Schwender J, Gemünden C, Lichtenthaler HK (2001) Chlorophyta exclusively use the 1-deoxyxylulose 5-phosphate/2-C-methylerythritol 4-phosphate pathway for the biosynthesis of isoprenoids. *Planta* 212:416-423

Scott JH, Neelson KH (1994) A biochemical study of the intermediary carbon metabolism of *Shewanella putrefaciens*. *J Bacteriol* 176:3408-3411

Seto H, Watanabe H, Furihata K (1996) Simultaneous operation of the mevalonate and non-mevalonate pathways in the biosynthesis of isopentenyl diphosphate in *Streptomyces aerioovifer*. *Tetrahedron Lett* 37:7979-7982

Sternberg LdSL, DeNiro MJ, Ajie HO (1986) Isotopic relationships between saponifiable lipids and cellulose nitrate prepared from red, brown and green algae. *Planta* 169:320-324

Sternberg LdSL (1988) D/H ratios of environmental water recorded by D/H ratios of plant lipids. *Nature* 333:59-61

Strauss G, Fuchs G (1993) Enzymes of a novel autotrophic CO<sub>2</sub> fixation pathway in the phototrophic bacterium *Chloroflexus aurantiacus*, the 3-hydroxypropionate cycle. *Eur J Biochem* 275:633-643

Summons RE, Jahnke LL, Roksandic Z (1994) Carbon isotopic fractionation in lipids from methanotrophic bacteria: Relevance for interpretation of the geochemical record of biomarkers. *Geochim Cosmochim Acta* 13:2853-2863

Summons RE, Franzmann PD, Nichols PD (1998) Carbon isotopic fractionation associated with methylotrophic methanogenesis. *Org Geochem* 28:465-475

Tagigiku R (1987) Isotopic and molecular indicators of origins of organic compounds in sediments. Ph.D. Thesis, Indiana University, Bloomington, Indiana, 248 p

Teece MA, Folge ML, Dollhopf ME, Neelson KH (1999) Isotopic fractionation associated with biosynthesis of fatty acids by a marine bacterium under oxic and anoxic conditions. *Org Geochem* 30:1571-1579

van der Meer MTJ, Schouten S, Sinninghe Damasté JS (1998) The effect of the reversed tricarboxylic acid cycle on the <sup>13</sup>C contents of bacterial lipids. *Org Geochem* 28:527-533

van der Meer MTJ, Schouten S, Rijpstra WIC, Fuchs G, Sinninghe Damasté JS (2001a) Stable carbon isotope fractionations of the hyperthermophilic crenarchaeon *Met-allosphaera sedula*. *FEMS Microbiol Lett* (in press)

van der Meer MTJ, Schouten S, van Dongen W, Rijpstra WIC, Fuchs G, Sinninghe Damasté JS, de Leeuw JW, Ward DM (2001b) Biosynthetic controls on the <sup>13</sup>C-contents of organic components in *Chloroflexus aurantiacus*. *J Biol Chem* (in press)

Vogler EA, Hayes JM (1978) The synthesis of carboxylic acids with carboxyl carbons of precisely known stable isotopic composition. *International Journal of Applied Radiation and Isotopes* 29:297-300

Vogler EA, Hayes JM (1979) Carbon isotopic fractionation in the Schmidt decarboxylation: evidence for two pathways to products. *J Org Chem* 44:3682-3686

White DW (1999) *The Physiology and Biochemistry of Prokaryotes*, 2<sup>nd</sup> edition. Oxford University Press, New York

Winters JK (1971) Variations in the natural abundances of <sup>13</sup>C in proteins and amino acids. Ph.D. Thesis, University of Texas, Austin, Texas, 76 p.

Yakir D (1992) Variations in the natural abundance of oxygen-18 and deuterium in plant carbohydrates. *Plant, Cell and Environment* 15:1005-1020

Yakir D, DeNiro MJ (1990) Oxygen and hydrogen isotope fractionation during cellulose metabolism in *Lemma gibba* L. *Plant Physiol* 93:325-332

Zelitch I (1975) Improving the efficiency of photosynthesis. *Science* 188:626-633

Zubay G (1998) *Biochemistry*, fourth edition. WCB/McGraw-Hill, New York